

PHYSICS OF STRANGE MATTER

Carsten Greiner^a and Jürgen Schaffner-Bielich^b

^a*Institut für Theoretische Physik, Universität Giessen, 35392 Giessen, Germany*

^b*Nuclear Science Division, Lawrence Berkeley National Laboratory, Berkeley, CA 94720, USA*

1 INTRODUCTION

All known nuclei are made of the two nucleons, the proton and the neutron. Besides those two lightest baryons there exist still a couple of other stable (but weakly decaying) baryons, the hyperons. These were found for the first time in cosmic ray experiments and were entitled as ‘strange’ because of their unusual long lifetimes of about 10^{-10} sec. For their notation in the hadron zoo of elementary particles one introduced the new quantum number ‘strangeness’ (or ‘hypercharge’). In the quark picture baryons are interpreted as being made out of three constituents, the quarks. Correspondingly the proton (uud) and neutron (udd) are made out of the two lightest quarks, the up and down quark. For the description of the hyperons a third flavour, the strange quark, was demanded. The lightest hyperon, the Λ -particle (uds), and the three Σ -particles (uus,uds,dds) contain one strange quark, the two more heavy Ξ -particles (uss,dss) contains two strange quark and the Ω -particle (sss) is solely made out of three strange quarks.

Up to now strangeness remains an experimentally as theoretically rather largely unexplored degree of freedom in strongly interacting baryonic matter. This lack of investigation reflects the experimental task in producing nuclei containing (weakly decaying) strange baryons, which is conventionally limited by replacing one neutron (or at maximum two) by a strange Λ -particle in scattering experiments with pions or kaons. There exist a broad knowledge about single hypernuclei, i.e. nuclei, where one nucleon is substituted by a Λ (or Σ) by means of the exchange reaction $\pi^+ + n \rightarrow \Lambda + K^+$ (the K^+ ($\bar{s}u$) denotes the positively charged kaon, the lightest strange meson). Over the last two decades a rich phenomenology has resulted for such hypernuclei.

However, there exist more or less no experimental insight how more than one hyperon behave inside a nuclei (or nuclear matter). The technical problem is to create within a tiny moment, smaller than the decay time of a hyperon,

enough hyperons and then to bring them together with nucleons to form any potential multi hypernuclei. By employing a relativistic shell model calculation, which gives a rather excellent description of normal nuclei and single Λ -hypernuclei, it was found that such configurations might exist as (small or large) bound multi hypernuclei (MEMO - metastable exotic multihypernuclear object). The reasoning for such exotic bound nuclei and the resulting extension of the periodic table to the strangeness degree of freedom will be discussed in detail in section 3.

Hypermatter could also be realized in a completely different picture. Indeed, this second and much more speculative possibility was raised by physicists much earlier. The fundamental theory of strong interactions, quantum chromodynamics, does not forbid the principle existence of 'larger' hadronic particles, so called multiquark states. Today only the mesons and baryons are known in nature. However, there could exist states with more than three quarks. Going further with this speculation one comes to the conclusion that only multiquark states with nearly the same number of up, down and strange quarks might exist as stable configurations. According to very schematic model calculations such states could exist as metastable or even absolutely stable objects, being then more bound than ^{56}Fe . Such a very speculative form of hypermatter is called strange quark matter. We will start our discussion with an introduction to the physics of strange quark matter in section 2.

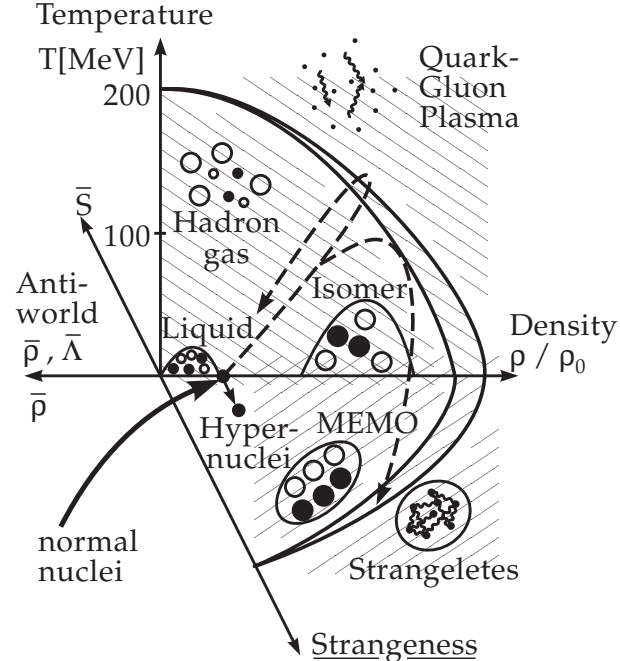


Fig. 1. Phase diagram of (hot) nuclear matter including the strangeness degree of freedom – MEMOs and possibly also strangelets establish as stable multistrange configurations.

Central (ultra-)relativistic heavy ion collisions provide the only source for the

formation of either multi-hypernuclear (strange hadronic matter) objects, consisting of nucleons, Λ 's and Ξ 's, or strangelets (strange multiquark droplets). To be more specific, on the average the occurrence of 20 Λ 's, 10 Σ 's and 1 Ξ 's per event for $Au(11.7\,AGeV)Au$ and of 60 Λ 's, 40 Σ 's and 5 Ξ 's per event for $Pb(160\,AGeV)Pb$ are expected to be created. In Fig. 1 we depict qualitatively what we want to elaborate in section 4: Customarily the equation of state of hot and dense hadronic matter (being created in a relativistic heavy ion collision) is characterized by means of a phase diagram ($\rho_B \leftrightarrow T$), where at some critical temperature and/or nonstrange baryon density eventually a phase transition to a deconfined quark gluon plasma (QGP) state does occur. However, the EOS to be passed through during a heavy ion collision incorporates also a new degree of freedom, the *net* strangeness (counting a surplus of strange over antistrange quarks). Like the occurrence of bound nonstrange nuclear matter, multihypernuclear matter, or small droplets (MEMOs) of this new state, may be revealed. In addition, also the phase transition to the deconfined state is affected by the possible conglomeration of the strangeness degree of freedom. In particular, if the strangelet does exist in principle, it has to be regarded as a cold, stable and bound manifestation of that phase being a remnant or ‘ash’ of the originally hot QGP-state. We will close section 4 in critically emphasizing the detection possibilities of such exotic states by their properties and lifetimes, also in respect to the present experimental undertaking at Brookhaven and at CERN.

In section 5 we finally want to give some insight on how the physics of strange matter can affect the physical picture of dense neutron stars.

2 STRANGE QUARK MATTER

The proposal that hypothetical strange quark matter droplets ('strangelets') at zero temperature and in β -equilibrium might be absolutely stable has stimulated substantial activity. Such a scenario would be of fundamental importance, as, for example, it could explain a large fraction of the non-observable mass of the universe in certain cosmological models, and could modify substantially our understanding of the structure and stability of neutron stars [1,2] (see also section 5).

Some years ago we proposed that such strange quark matter droplets might as well play an important role in ultrarelativistic heavy-ion collisions [3–5]. One important goal in ultrarelativistic heavy-ion physics is the observation of a temporarily created quark gluon plasma. An enhanced production of strange particles from the QGP, especially an enhanced K^+/π^+ -ratio [6], and the J/ψ -suppression [7] were proposed as possible signatures for such a novel state of deconfined, strongly interacting matter. It was subsequently shown, however, that such indications, as indeed were experimentally found, can be still understood as being due to the formation of a very (energy-) dense and hot region of matter consisting of confined hadrons or precursor effects of QGP formation. Therefore, it seems that perhaps the only unambiguous way to detect the transient existence of a QGP might be the experimental observation of exotic remnants ('ashes' of the QGP), like the formation of strange quark matter droplets. To this interesting aspect we will turn back in section 4.

In this first section we now summarize the reasons for the speculation of (cold) stable or metastable strange quark matter in the bulk. In addition, being more relevant for heavy ion physics, also a brief description of finite pieces of strange quark matter will be given (see also section 4).

Strange quark matter or strangelets are thought to be confined (bulk) objects containing a large number of delocalized quarks ($u\dots u$, $d\dots d$, $s\dots s$), so-called multiquark droplets. Multiquark states consisting only of u- and d-quarks must have a mass larger than ordinary nuclei, otherwise normal nuclei would certainly be unstable, which, of course, is not the case. However, the situation is different for droplets of SQM, which would contain approximately the same amount of u-, d- and s-quarks. Bodmer was the first person to consider this new form of matter [8]; he proposed that strange multiquark clusters, being much more compressed than ordinary nuclei, may exist as long-lived exotic isomers of nuclear matter inside neutron stars.

Chin and Kerman [9] and independently McLerran and Bjorken [10] postulated two reasons why such huge hadronic states should be relatively stable:

- (1) The (weak) decay of a s-quark into a d-quark would be suppressed or

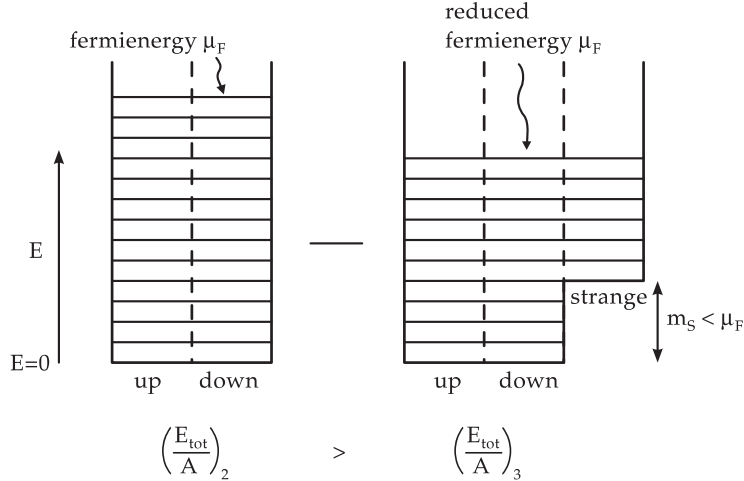


Fig. 2. Schematic illustration of the energy levels inside a multiquark bag with two or three flavours.

forbidden because the lowest single particle states are occupied.

(2) The strange quark mass is lower than the Fermi energy of the u- or d-quark in such a quark droplet; the opening of a new flavour degree of freedom tends to lower the Fermi energy and hence also the mass of the strangelet (see Fig. 2).

According to this picture, SQM should appear as a nearly neutral and massive state because the number of strange quarks is nearly equal to the number of massless up or down quarks and so the strange quarks neutralize that hypothetical form of nuclear matter.

It was then later Witten who realized and hence raised the intriguing possibility that strange quark matter might in principle also be absolutely stable and may also provide an explanation for *cold dark matter* in the universe [11]. This would be the case if the mass of a strangelet is smaller than the mass of the corresponding ordinary nucleus with the same baryon number and hence be the true groundstate of nuclear matter! If being stable and nearly neutral, it could exist at *all possible sizes* [12], as the small Coulomb energy is not sufficient for a break up into smaller pieces [13]. Such a speculation is illustrated in Fig. 3 [14].

Presently such a highly speculative scenario cannot be ruled out. Normal nuclei could only transform into these novel states by a higher order weak decay; the decay into one single Λ -particle would be energetically forbidden. The time-scale for such collective decays is extremely large; accordingly, normal nuclei would remain intact.

On the other hand, it is also conceivable that the mass per baryon of a strange droplet is lower than the mass of the strange Λ -baryon, but larger than the nucleon mass. The droplet is then in a metastable state, it cannot

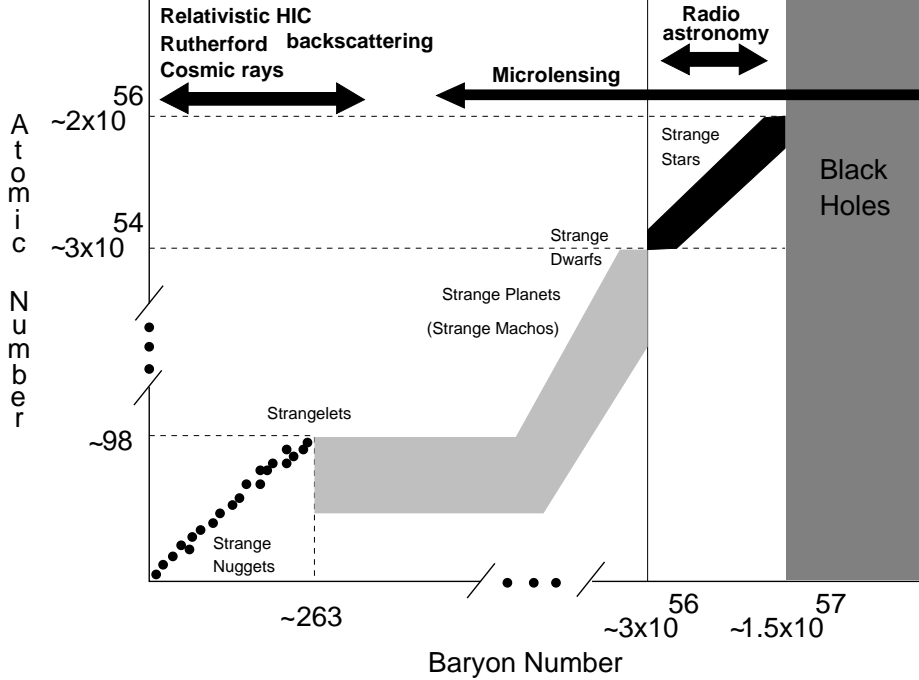


Fig. 3. The possible places where to find stable strange quark matter. If being absolutely stable SQM might exist in forms of small nuggets (strangelets) being not (much) larger than normal nuclei. It might also span as a charge neutral state the empty ‘nuclear desert’ [12] within the range from $A_B \sim 300$ up to sizes of neutron stars $A_B \sim 10^{56}$.

decay (strongly) into Λ ’s [9].

For a very simple quantification of these ideas one typically models quark matter in *bulk* by a Fermi gas equation of state of interacting quarks which to first order in $\alpha_c = g^2/16\pi$ is given by [15]

$$\Omega_i(m_i, \mu_i) = -\frac{1}{4\pi^2} \left(\mu_i(\mu_i^2 - m_i^2)^{1/2} \left(\mu_i^2 - \frac{5}{2}m_i^2 \right) + \frac{3}{2}m_i^4 \ln \frac{\mu_i + (\mu_i^2 - m_i^2)^{1/2}}{m_i} \right. \\ \left. - \frac{8}{\pi} \alpha_c \left[3 \left(\mu_i(\mu_i^2 - m_i^2)^{1/2} - m_i^2 \ln \frac{\mu_i + (\mu_i^2 - m_i^2)^{1/2}}{m_i} \right)^2 - 2(\mu_i^2 - m_i^2) \right] \right) . \quad (1)$$

Here m_i and μ_i denote the (current) mass and the chemical potential, respectively, of the quark flavour $i=u,d,s$. For the total potential the vacuum excitation energy BV has to be added, which corresponds to the energy difference between the ‘false’, perturbative vacuum inside the ‘bag’ and the true

vacuum at the outside, and which, in return, confines the quarks, i.e.

$$\Omega(\mu_q, \mu_s, m_s; \alpha_c) = \sum_{i=u,d,s} \Omega_i(m_i, \mu_i) + BV . \quad (2)$$

$m_u \approx m_d \approx 0$ and $\mu_u = \mu_d$ has been implicitly taken for an isospin symmetric situation. From this expression (2) the energy per baryon in the groundstate can be readily obtained by varying E/A with respect to the baryon density to describe the system at zero pressure. To fix the amount of net strangeness in the system the strangeness fraction f_s is introduced as the ratio of net strangeness and total baryon number, i.e.

$$f_s = \frac{n_s - n_{\bar{s}}}{\frac{1}{3} [(n_q - n_{\bar{q}}) + (n_s - n_{\bar{s}})]} \stackrel{T=0}{\equiv} N_s/A_B . \quad (3)$$

Fig. 4. Energy per baryon for strange quark matter at zero temperature and zero pressure, as a function of the strangeness fraction f_s . The dashed line defines the corresponding mass of a hyperonic matter ground-state.

The energy per baryon of quark matter in the groundstate thus depends solely on the explicit strangeness fraction f_s and on the three intrinsic parameter, the strange (current) mass m_s , the coupling constant α_c and the bag constant $B^{1/4}$. For most purposes to come a non-zero α_c can be ‘absorbed’ by a slight increase in the bag parameter. In Fig. 4, E/A is depicted as a function of f_s and vanishing coupling constant, but for various choices of the bag constant and the strange quark mass. The minimum in the energy is achieved for a

strangeness fraction $f_s \sim 0.7$, if the more popular and smaller mass $m_s = 150$ MeV is taken. According to the formula $Z/A = (1 - f_s)/2$ smaller pieces of strange quark matter would then be slightly positive at its most stable position. A necessary condition for the stability of strange quark matter against strong decay is that its energy per baryon must be smaller than that of the corresponding hyperonic matter (dashed-dotted curve), which can be determined as

$$\begin{aligned} m_{Hyp} &= f_s m_\Lambda + (1 - f_s) m_N - \epsilon_B & ; & \quad 0 \leq f_s \leq 1 \\ (f_s - 1) m_\Xi + (2 - f_s) m_\Lambda - \epsilon_B & & ; & \quad 1 \leq f_s \leq 2 \\ (f_s - 2) m_\Omega + (3 - f_s) m_\Xi - \epsilon_B & & ; & \quad 2 \leq f_s \leq 3 \end{aligned} \quad (4)$$

where Λ , Ξ and Ω are the masses of the strange hyperons and ϵ_B is the binding energy per nucleon, which is, for simplicity, taken to be the infinite nuclear matter parameter of 16 MeV.

If popular parameters within bag models, like the MIT bag model employed here, are extrapolated to strange quark droplets, both of the above considered pictures turn out to be possible. However, metastable strangelets relax somewhat the stringent conditions on the choice of parameters of the bag model required by an absolutely stable state [13], namely small Bag constants $B^{1/4} \lesssim 150$ MeV (which, within the same model extrapolated to finite temperatures, would give a too low critical transition temperatures $T_c \sim 100$ MeV for the onset of deconfinement). For large pieces of absolutely stable strange matter one has to include the Coulomb effect due to the still tiny net positive charge [13]. These have been neglected in the present figure 4. It turns out that then the minimum of the energy per baryon number will be shifted smoothly to $f_s \rightarrow 1$ instead of $f_s \approx 0.7$, so that the strange matter piece still carries a very small positive charge.

On the other hand, from Fig. 4 it follows that for bag parameters $B^{1/4}$ lower than 190 MeV strange quark droplets can only decay via weak interactions, i.e., they would be *metastable*. The baryon density of a strangelet would be about 1.5 – 2 of normal nuclear matter density. For larger B-values (large) strangelets are instable.

The idea of the existence of metastable strangelets was actually raised earlier than the possibility of a new groundstate of normal nuclear matter. Chin and Kerman [9] had employed the original favoured MIT bag parameters of $B^{1/4} = 145$ MeV, $g_c^2/4\pi = 2.2$ ($\alpha_c = 0.55$) and a strange quark mass of about $m_s = 279$ MeV [16,17]. The minimum they find is shifted to a higher strangeness content. In quark matter one-gluon exchange is repulsive, if the quarks are massless and relativistic, and attractive if the quarks are massive and behave already nonrelativistic. Accordingly, metastable strange quark matter in the ground state might as well be slightly negatively charged. (This

cannot be the case if it would exist in absolutely stable form, for than, normal, positively charged nuclei would be attracted and absorbed at the surface. Such catastrophic consequences have to be excluded.) One should remark, however, that the linear expansion to obtain the expression for E/A used in Ref. [9] is not valid, as the energy density as well as the baryon density turn negative for $\alpha_c > \pi/8$, so that a perturbative expansion is meaningless and signals the breakdown of perturbation theory. This basically sheds some light how ‘seriously’ the calculations, the conclusions and the speculations have to be taken!

Originally (strange) quark matter in bulk was thought to exist only in the interior of neutron stars where the pressure is as high that the neutron matter melts into its quark substructure [18,19,15] (see also section 5). In Witten’s prospective scenario hot strange quark matter nuggets could have condensed out of the deconfined phase during the phase transition in the expanding and cooling early universe [11]. These would carry most of the tiny surplus in baryon number of the whole universe. The baryon number would remain inside if the heat and entropy of the nuggets is carried away mainly by neutrino emission instead of mesons and especially baryons. If an absolutely stable groundstate would exist, i.e. if *cold* strange quark matter is the true groundstate of nuclear matter, the hot nuggets would further cool and instead of suffering a complete hadronization they might settle into these new states and hence could resolve the dark matter problem. Since then the idea of absolute stability has stimulated a lot of work on potential consequences in astrophysics [2,20].

Nuclear collisions, however, do allow also the detection and study of only short lived, metastable strangelets, which will decay by flavour changing weak processes. Most of the experiments are sensitive to strangelets with lifetimes up to $10^{-8} - 10^{-9}$ sec. In addition, the strangelets to be expected will be small. Hence, in the last part of this subsection, we already address the potential importance of *finite* size effects. Later in section 4 we come back to this analysis in somewhat more detail in order to try to pin down possible short-lived or long-lived candidates for the present and future experimental undertakings. Due to these effects and the wider range of employed phenomenological parameters, smaller strangelets, if they exist, are more likely to be metastable than being absolutely stable.

Small pieces of (strange) quark matter are described within a spherical MIT-bag by filling up the bag with exact single-particle Dirac-states [13,21,4]. These calculations have been done with $\alpha_c = 0$. The first MIT boundary condition, which ensures confinement, is basically a Bogolyubov-type condition for the scalar mass of the quark, i.e. $M(r > R_{bag}) \rightarrow \infty$, and leads to the following equation for the single particle energies:

$$j_{l_\kappa}(pR) = -\text{sign}(\kappa) \frac{p}{E + m_i} j_{l_{-\kappa}}(pR) \quad (5)$$

with

$$p = \frac{\omega_{\kappa,\alpha}^i}{R} \quad (6)$$

$$E_{\kappa,\alpha}^i = \left(\left(\frac{\omega_{\kappa,\alpha}^i}{R} \right)^2 + m_i^2 \right)^{\frac{1}{2}}$$

Here m_i is the quark mass ($i=u,d,s$), with $m_u = m_d = 0$ MeV and $m_s = 150$ MeV. R defines the radius of the bag, κ is the angular momentum quantum number and α labels the eigenvalues in this quantum state κ . The total energy of the finite system is obtained by summing the ‘lowest’ energy eigenvalues and adding the phenomenological bag energy BV for the perturbative vacuum:

$$E_{total} = \sum_{i=u,d,s} \sum_{\kappa; \alpha}^{E_{\kappa,\alpha}^i \leq \mu_i} N_\kappa E_{\kappa,\alpha}^i + B \left(\frac{4\pi}{3} R^3 \right) , \quad (7)$$

where the degeneracy $N_\kappa = 6|\kappa|$. In addition, a center of momentum correction and a Coulomb term $((N_0 - 2N_s)/R)^2/60\alpha$ is included. (In the original MIT model [16] a zero-point energy term of the form $-Z_0/R$ is also included as a more or less phenomenological parameter for fitting the light hadron spectra. Such an additional attractive term may have some noticeable effect on very small strangelets.) The volume V or the radius R , respectively, has to be chosen in a way that the total pressure of the quarks inside the bag compensates the vacuum pressure B , or, in other words, $\partial E_{total}/\partial R = 0$.

Fig. 5 shows the dependence of the energy per baryon of a giant bag on the baryon number for $B^{\frac{1}{4}} = 145$ MeV and for a (constant) strangeness fraction of $f_s = 1$, i.e. SU(3) symmetric and charge neutral matter. One clearly sees a pronounced shell structure. Especially the first magic number shows up nicely at a baryon number of 6, that is, if all quarks completely fill the $1S_{1/2}$ ground state (the so called ‘quark-alphas’ [22]). Generally speaking, the energy per baryon for a smaller strangelet with a baryon number $N_B < 50$ is about 50-100 MeV/N larger as compared to the infinite quark matter calculations. This can be interpreted in terms of a surface correction [13]. If one varies the number of up and down and strange quarks, strangelets do have a large variety of nearly degenerate states. This fact is interesting for the heavy ion experiments because these nearly degenerate states will be stable against strong decay and thus would all be detectable if their lifetime against weak decay is long enough (see section 4).

We close this section with some cautionary remarks:

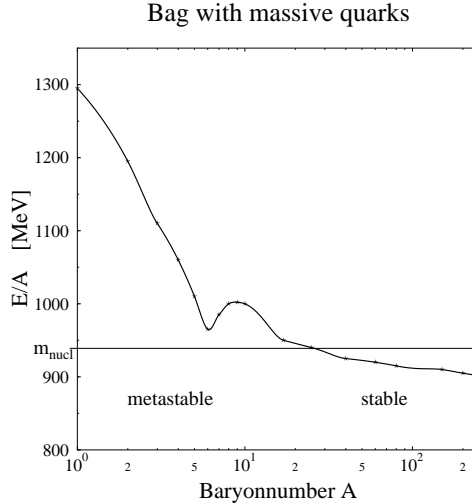


Fig. 5. E/A versus A in a hadronic (MIT-)Bag model for noninteracting quarks. A constant strangeness fraction $f_s=1$, i.e. $N_u = N_d = N_s$, is assumed ($m_s = 150$ MeV, $B^{\frac{1}{4}} = 145$ MeV).

- The existence of strange quark matter cannot rigorously be predicted by theory, although some general and appealing arguments for its stability do exist. A detailed understanding cannot be achieved by employing more or less relatively simple, phenomenological models. Ultimately only the experimentalists (in astrophysics or heavy ion physics) may prove its existence or nonexistence.
- For smaller strangelets, as the above calculations suggest, finite size effects and a profound shell structure might be quite important. For very small strangelets the colour magnetic part of the gluon exchange should be important and should further favour SU(3) symmetric multiquark states to exist. In this respect the prominent H-Dibaryon proposed by Jaffe [23] would be the smallest strangelet.
- Although the idea of absolute stable pieces of strange quark matter is intriguing in its consequences for astrophysics, metastable strangelets only need to be smaller in mass than the corresponding hyperonic multi-baryon configuration, which is much higher than that of a normal nuclei. Because of this argument it might well be that (small) strangelets, if they do exist, are metastable and not absolutely stable (see section 4).

3 STRANGE HADRONIC MATTER

Strange hadronic matter consists of baryons, i.e. nucleons and hyperons as quasiparticles are the basic constituents. In this case, there exists some knowledge about the properties of hyperons inside nuclei from hypernuclear physics up to two units of strangeness. They extend the chart of nuclides to a third dimension in addition to baryon number and isospin. The extension to it will open new perspectives for nuclear physics. This is what we are going to discuss in the following subsections.

First we will give a short introduction to hypernuclear physics. Then we list all possible metastable combinations of nucleons and hyperons on the basis of symmetry considerations which are stable against strong interactions. If they are bound, they will have lifetimes of the order of the weak decay lifetime of the hyperons of 10^{-10} s.

The extrapolation to systems with a large amount of strangeness will rely then on several basic features: the knowledge that the Λ -nucleon and the $\Lambda\Lambda$ interaction is attractive, the existence of metastable combinations of nucleons and hyperons or hyperons alone, and the effect of the Pauli-blocking in the hyperon world.

The properties of strange hadronic matter are then discussed on the basis of the relativistic mean field model, which is able to reproduce fairly well the properties of nuclei and hypernuclei. Here we will focus on the properties of superheavy elements. As the hyperons Σ^- and Ξ^- are negatively charged, a similar situation as for strangelets occur and superheavy elements with $A > 250$ and a low charge are possible.

3.1 *Hypernuclei*

Our intention is not to give a detailed overview about hypernuclear physics, as there exist excellent reviews in the literature [24,25], but to give a short summary of the main features.

Hypernuclei are known since 1953 as Danysz and Pniewski observe the first Λ -hypernuclei in a cosmic ray emulsion experiment [26] (in some of the older publications hypernuclei are called hyperfragments). In the following decades one has found Λ -hypernuclei up to a maximum mass number of $A = 15$ which is due to the resolution of emulsion experiments. The lightest one is the hypernucleus $^3_\Lambda\text{H}$, a system of one proton, one neutron and one Λ . Another interesting fact is the existence of the hypernucleus $^9_\Lambda\text{Be}$: the presence of the Λ glues together and stabilizes the nuclear core ^8Be which normally decays

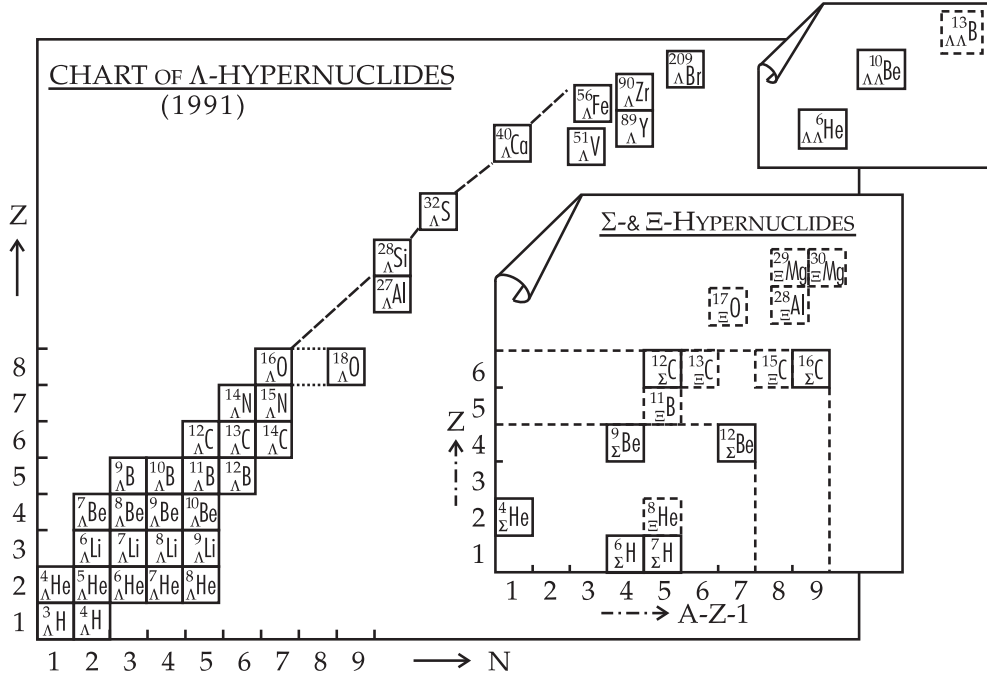


Fig. 6. The chart of Λ hypernuclei as well as Ξ , Σ and double Λ hypernuclei known so far (taken from [25]).

to two α -particles! Other examples for the enhanced stability of hypernuclear systems compared to their nuclear cores are the hypernuclei $^9_{\Lambda}Li$ and $^9_{\Lambda}B$. We will present even more impressive ones in the forthcoming sections.

In the 70's programs started at the AGS [27] and at CERN [28] for detecting Λ -hypernuclei by using meson beams and spectroscopy techniques. Here one uses the reaction:



A special feature of this reaction is, that there exist a magic momentum of the ingoing kaon where the Λ is produced at rest inside the nucleus facilitating the formation of a bound hypernuclear system. Another generation of hypernuclear spectroscopy uses the reverse reaction:



This reaction yields a lower resolution, but deep lying states can be detected more easily [29]. The study of these reactions started in the 80's at the AGS [30,31] and at the KEK in Japan [32].

The hypernuclear chart with the hypernuclear states is shown in Fig. 6. Experimentally one has seen hypernuclei up to a baryon number of $A = 209$

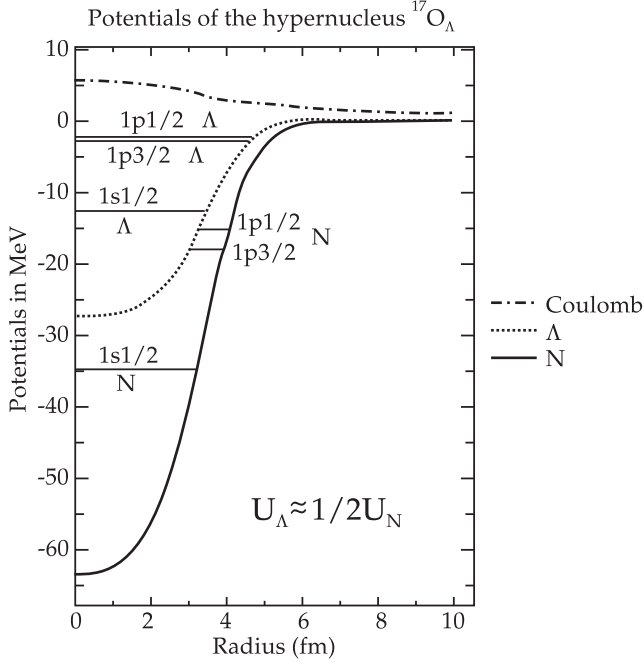


Fig. 7. The potentials and the single particle levels for the hypernucleus $^{17}\Lambda\text{O}$ in the RMF model.

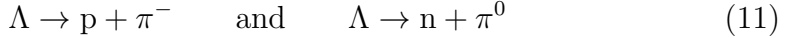
(Tungsten) where one neutron is replaced by a Λ . Moreover one is able to extract the single particle binding energies from excited states (like $1f_\Lambda$) to very deep lying states $1s_\Lambda$ which opens the possibility to study deeply bound probes inside the nucleus over a wide range of mass number. This was an excellent test (and success) of the shell model [33]. An essential feature of the Λ -nucleon interaction is that one has seen no spin-orbit splitting experimentally, which leads to the statement that the Λ behaves as a spinless neutron [28,34] (a theoretical discussion of this topic can be found in [35]). The potential depth of the Λ in nuclear matter can be derived from the experimental data to be

$$U_\Lambda^{(N)} = 27 - 30 \text{ MeV} \quad (10)$$

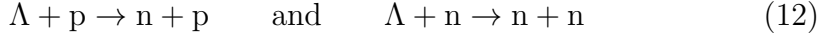
which has to be compared with the corresponding nuclear depth of about 60 MeV. Calculations using Hartree-Fock models [36] and Relativistic Mean-Field (RMF) models [37–42] are able to reproduce very nicely the observed trend of the single particle energy with the mass number.

Fig. 7 shows as an example a calculation for the hypernucleus $^{17}\Lambda\text{O}$. The potential for the Λ is shallower than for the nucleon but of a similar radius. The 1s state of the Λ is a separate state within this Λ potential. The surface thickness is bigger for the Λ density distribution than for the nucleons. This will cause a Λ -halo as the Λ is not as deeply bound as the nucleons. The single particle energies for the 1p states of the Λ are very close to each other, resembling the weak spin-orbit force of the Λ -nucleon interaction.

The lifetime of the hypernuclei has been also measured. They decay weakly by emission of a pion (mesonic decay channel):



like the free Λ releasing 38 and 41 MeV, respectively. Moreover a new reaction, the nonmesonic decay, opens in the nuclear medium



which releases an energy of about 177 MeV. The mesonic channel is dominant for very light systems but it is negligible for heavier hypernuclei like the hypernucleus $^{12}\Lambda\text{C}$ [43]. This results from the dominant absorption of the pion inside the nucleus and of the larger phase space for the nonmesonic decay. Finally, the lifetime of Λ -hypernuclei has been determined to be at the order of 10^{-10} s even for $A \approx 200$ [44], which is close to the lifetime of the Λ in free space.

There exists also some scarce information about Σ - and Ξ -hypernuclei. The experimental situation concerning the existence of bound Σ -hypernuclear systems is still controversial. The strong process $\Sigma + N \rightarrow \Lambda + N$ smears out possible peaks in the meson spectra. Nevertheless, one has found surprisingly small structures in hypernuclear spectra. All these structures are lying in the continuum. Recent analysis of the data about Σ^- -atoms indicate that the isoscalar potential depth of a Σ in a bath of nucleons in its groundstate is repulsive [45] which would prevent a formation of bound Σ hypernuclear states. The isovector potential can be attractive, as for example in light systems like $^4\text{He}\Sigma^+$ and might form a bound state. Indications for such a bound state have been seen in [46].

Ξ -hypernuclei have already been found shortly after the first observation of a Λ -hypernucleus in emulsion experiments using kaon beams. There exist seven emulsion events in the literature (for a review see [47]) showing that the strong conversion process $\Xi + N \rightarrow \Lambda + \Lambda$ still allows for bound systems. The potential depth of a Ξ in nuclear matter has been derived by using Wood-Saxon potentials to be

$$U_{\Xi}^{(N)} = 21 - 24 \text{ MeV} \quad (13)$$

whereas relativistic mean field calculations get a little higher value of $U_{\Xi}^{(N)} = 28 \text{ MeV}$ [48].

There exist also three $\Lambda\Lambda$ -hypernuclear events by caption of a Ξ^- and a detection of their mesonic decays (for an excellent review see [49]). In particular

Hypernucleus	$B_{\Lambda\Lambda}$ [MeV]	$\Delta B_{\Lambda\Lambda}$ [MeV]
$^6_{\Lambda\Lambda}\text{He}$	10.9 ± 0.6	4.7 ± 0.6
$^{10}_{\Lambda\Lambda}\text{Be}$	17.7 ± 0.4	4.3 ± 0.4
$^{13}_{\Lambda\Lambda}\text{B}$	27.5 ± 0.7	4.8 ± 0.7

Table 1

The two observables $\Delta B_{\Lambda\Lambda}$ and $B_{\Lambda\Lambda}$ of the known double Λ -hypernuclei.

these are the hypernuclei $^6_{\Lambda\Lambda}\text{He}$ [50], $^{10}_{\Lambda\Lambda}\text{Be}$ [51], and $^{13}_{\Lambda\Lambda}\text{B}$ [52,53]. These data constitute our only (and poor) knowledge about the hyperon-hyperon interactions. One defines the following two quantities:

$$\begin{aligned} B_{\Lambda\Lambda}(^A_{\Lambda\Lambda}Z) &= B_\Lambda(^A_{\Lambda\Lambda}Z) + B_\Lambda(^{A-1}_\Lambda Z) \\ \Delta B_{\Lambda\Lambda}(^A_{\Lambda\Lambda}Z) &= B_\Lambda(^A_{\Lambda\Lambda}Z) - B_\Lambda(^{A-1}_\Lambda Z) \end{aligned} \quad (14)$$

where $B_{\Lambda\Lambda}$ is the sum of the binding energies of the two Λ 's and $\Delta B_{\Lambda\Lambda}$ is a measure of the $\Lambda\Lambda$ interaction. The experimental values are listed in table 1. The $\Lambda\Lambda$ interaction is attractive and relatively strong. The value of 4–5 MeV has to be contrasted with the corresponding values of 6–7 MeV for the NN interaction and 2–3 MeV for the ΛN interaction.

Hence, the $\Lambda\Lambda$ interaction is much stronger than the ΛN interaction and about 3/4 of the NN interaction. This has to be taken into account for hyperon-rich systems.

3.2 Classification of Strange Hadronic Matter

The strong interaction conserves strangeness and charge and the baryon number. Therefore combinations of nucleons and hyperons, which are stable against weak interactions, so called metastable combinations, have to be classified according to these quantum numbers.

First, in a nuclear environment, strong reactions in the medium among different baryon species can occur. There exist two strong reactions, which have a considerable lower mass difference (or Q-value) as the others: $\Xi^- + p \rightarrow \Lambda + \Lambda$ and $\Xi^0 + n \rightarrow \Lambda + \Lambda$, releasing 28 and 23 MeV energy, respectively. Indeed these two reactions will play a major role in the discussion of bound strange hadronic systems and we will keep them in mind. All other reactions have a rather large Q-value of more than 50 MeV which can not be overcome by binding energy differences (remember that the maximum binding of a nucleon is about 60 MeV). Nevertheless, the final products of all reactions constitutes the combinations of two different species which are for a given charge and strangeness the deepest lying state and which are therefore stable against strong interac-

$-S \setminus Z$	-2	-1	0	+1	+2
0			nn	np	pp
1		$\Sigma^- n$	Λn	Λp	$\Sigma^+ p$
2	$\Sigma^- \Sigma^-$	$\Xi^- n$	$\Lambda \Lambda$	$\Xi^0 p$	$\Sigma^+ \Sigma^+$
3	$\Xi^- \Sigma^-$	$\Xi^- \Lambda$	$\Xi^0 \Lambda$	$\Xi^0 \Sigma^+$	
4	$\Xi^- \Xi^-$	$\Xi^0 \Xi^-$	$\Xi^0 \Xi^0$		
5	$\Xi^- \Omega^-$	$\Xi^0 \Omega^-$			
6	$\Omega^- \Omega^-$				

Table 2

The possible configurations of metastable partners of nucleons and hyperons classified according to their total strangeness S and charge number Z .

$-S \setminus Z$	-2	-1	0	+1	+2
1				Λnp	
2					
3	$\Xi^- \Sigma^- n$	$\Xi^- \Lambda n$		$\Xi^0 \Lambda p$	$\Xi^0 \Sigma^+ p$
4					
5		$\Xi^- \Xi^0 \Lambda$			
6					
7	$\Omega^- \Xi^- \Xi^0$				

Table 3

The possible configurations of metastable combinations of three different baryon species classified according to their total strangeness S and charge number Z .

tions. All possible metastable combinations of two different species are listed in table 2. Next consider a composite system of an arbitrary number of nucleons and hyperons. One can easily see, that the stability against strong interactions does not depend on the number of baryons, e.g. on the number of neutrons or Σ^- 's for the combination $\{n, \Sigma^-\}$. Therefore our considerations of metastability are valid for an arbitrary number of respective baryons. Note that we only study the stability against strong interactions here. Whether the combination is indeed bound or not will be discussed afterwards.

Next one can think of metastable combinations of three or even more different species. The former ones are listed in table 3. Of special interest is that systems consisting of $\{\Lambda, \Xi^0, \Xi^-\}$ -hyperons are metastable (they form purely hyperonic matter to be discussed later). More than three different baryon species can not form a metastable combination in free space as one can see from this table. For a metastable object of four different baryon species every combination of

three of them must be one of the metastable triplets given in table 3. As this can not be the case there does not exist metastable combinations of more than three different baryons in free space. The situation changes if one introduces interactions which will be presented in the following section.

3.3 Relativistic Mean-Field Model

In the preceding sections we have discussed the input for a theoretical description of strange hadronic matter. In the following we present an extended relativistic mean field model which is able to reproduce fairly well the experimental data of nuclei and hypernuclei and implements all hyperons. For reviews about this model for finite nuclei see [54,55].

The basic idea of this approach is the meson-exchange picture, where baryons interact via the exchange of mesons, usually a scalar meson σ which parametrizes effectively the two-pion exchange [56], the vector meson ω (hereafter the field V_μ) and the isovector meson ρ (field \vec{R}_μ) for isotopic trends. One starts from the Lagrangian

$$\mathbf{L} = \mathbf{L}_{\text{Baryon}} + \mathbf{L}_{\text{Meson}} + \mathbf{L}_{\text{Coupling}} + \mathbf{L}_{\text{Coulomb}} \quad (15)$$

with free terms for the baryon and meson fields

$$\mathbf{L}_{\text{Baryon}} = \sum_B \bar{\Psi}_B (i\gamma^\mu \partial_\mu - m_B) \Psi_B \quad (16)$$

$$\mathbf{L}_{\text{Meson}} = \frac{1}{2} \partial^\mu \sigma \partial_\mu \sigma - U(\sigma) - \frac{1}{4} G^{\mu\nu} G_{\mu\nu} + \frac{1}{2} m_\omega^2 V^\mu V_\mu \quad (17)$$

$$- \frac{1}{4} \vec{B}^{\mu\nu} \vec{B}_{\mu\nu} + \frac{1}{2} m_\rho^2 \vec{R}^\mu \vec{R}_\mu \quad (18)$$

where the sum runs over all baryons of the baryon octet ($p, n, \Lambda, \Sigma^+, \Sigma^0, \Sigma^-, \Xi^0, \Xi^-$). The term $U(\sigma)$ stands for the scalar selfinteraction

$$U(\sigma) = \frac{1}{2} m_\sigma^2 \sigma^2 + \frac{b}{3} \sigma^3 + \frac{c}{4} \sigma^4 \quad (19)$$

which has been introduced by Boguta and Bodmer [57] to get a correct compressibility of nuclear matter. Another stabilized functional form has been given by Reinhard [58]. The interaction is introduced by a minimal coupling of meson fields and baryon bilinear forms

$$\mathbf{L}_{\text{Coupling}} = - \sum_B g_{\sigma B} \bar{\Psi}_B \Psi_B \sigma \quad (20)$$

$$- \sum_B g_{\omega B} \bar{\Psi}_B \gamma^\mu \Psi_B V_\mu \quad (21)$$

$$- \sum_B g_{\rho B} \bar{\Psi}_B \gamma^\mu \vec{\tau}_B \Psi_B \vec{R}_\mu \quad . \quad (22)$$

For finite nuclei one takes also account of the coulomb force

$$\mathbf{L}_{\text{Coulomb}} = - \frac{1}{4} F^{\mu\nu} F_{\mu\nu} - \sum_B q_B e \bar{\Psi}_B \gamma_\mu \Psi_B A^\mu \quad (23)$$

where q_B is the charge number of the baryon. We have used here the following notation

$$\begin{aligned} G^{\mu\nu} &= \partial^\mu V^\nu - \partial^\nu V^\mu \\ \vec{B}^{\mu\nu} &= \partial^\mu \vec{R}^\nu - \partial^\nu \vec{R}^\mu + i \vec{R}^\mu \times \vec{R}^\nu \\ F^{\mu\nu} &= \partial^\mu A^\nu - \partial^\nu A^\mu \quad . \end{aligned} \quad (24)$$

The equations of motions can be derived in the standard way

$$\partial_\nu \frac{\partial \mathbf{L}}{\partial (\partial_\nu q_i)} - \frac{\partial \mathbf{L}}{\partial q_i} = 0, \quad q_i = \sigma, V_\mu, R_\mu, A_\mu, \Psi_B, \bar{\Psi}_B \quad (25)$$

and one gets Klein-Gordon and Proca equations for the meson fields with source terms coming from the baryon fields

$$(\partial_\mu \partial^\mu + U'(\sigma)) \sigma = - \sum_B g_{\sigma B} \bar{\Psi}_B \Psi_B \quad (26)$$

$$\partial^\mu G_{\mu\nu} + m_\omega^2 V_\mu = \sum_B g_{\omega B} \bar{\Psi}_B \gamma_\mu \Psi_B \quad (27)$$

$$\partial^\mu \vec{R}_{\mu\nu} + m_\rho^2 \vec{R}_\mu = \sum_B g_{\rho B} \bar{\Psi}_B \vec{\tau}_B \gamma_\mu \Psi_B \quad (28)$$

where

$$U'(\sigma) = \frac{\partial}{\partial \sigma} U(\sigma) \quad . \quad (29)$$

The equation for the electromagnetic field reads

$$\partial^\mu F_{\mu\nu} + m_\omega^2 A_\mu = q_B e \bar{\Psi}_B \gamma_\mu \Psi_B \quad . \quad (30)$$

The Dirac equation for each baryon

$$\left\{ i\gamma^\mu \partial_\mu + m_B + g_{\sigma B} \sigma + g_{\omega B} \gamma^\mu V_\mu + g_{\rho B} \gamma^\mu \vec{\tau}_B \vec{R}_\mu + q_B e \gamma^\mu A_\mu \right\} \Psi_B = 0 \quad (31)$$

contains now potential terms from the meson and coulomb fields. The scalar field shifts the mass to the effective mass defined as

$$m_B^* = m_B + g_{\sigma B} \sigma \quad . \quad (32)$$

Analogously, the vector fields shift the energy and momentum of the baryon. The equations (26)-(30) and (31) constitute a set of coupled differential equations which have to be simplified in order to solve them. In the following we will use the relativistic mean field (RMF) approximation, where the meson fields (and the Coulomb field) are replaced by their classical expectation values

$$\sigma \rightarrow \langle \sigma \rangle, \quad V_\mu \rightarrow \langle V_\mu \rangle, \quad \vec{R}_\mu \rightarrow \langle \vec{R}_\mu \rangle, \quad A_\mu \rightarrow \langle A_\mu \rangle \quad (33)$$

i.e. quantum fluctuations of these fields are neglected. Furthermore the many body wavefunctions of the baryons are treated on the Hartree-level. They are approximated by a sum of single particle wave functions

$$\Psi_B = \sum_\alpha a_{\alpha, B}^+ \psi_{\alpha, B} \quad , \quad (34)$$

where the sum runs only over the occupied states. The contribution coming from the Dirac-sea is therefore also neglected (this is the no-sea approximation). Note that in the so called relativistic Hartree-approximation (RHA) the quantum fluctuations coming from the Dirac-sea are implemented by renormalizing the Lagrangian [56] which we will not discuss here. It is important to know that all non-diagonal coupling terms vanish in the relativistic mean field approximation or at the Hartree-level. They contribute at the next order which takes into account the Fock-term (this is the Dirac-Hartree-Fock approximation). The coupling term to the pseudoscalar fields (pion and kaon fields) and pseudovector fields vanishes in the RMF approximation due to the γ_5 matrix which mixes upper and lower components of the wave functions. Also only the third component of the isovector field is present in the RMF approximation.

For spherical and static systems (nuclei in its groundstate) the fields do only depend on the radius

$$\sigma = \sigma(|\vec{r}|), \quad V_\mu = \delta_{\mu 0} V_0(|\vec{r}|), \quad \vec{R}_\mu = \delta_{\mu 0} \delta_{i0} R_{0,0}(|\vec{r}|), \quad A_\mu = \delta_{\mu 0} A_0(|\vec{r}|) \quad (35)$$

and the spatial components of the vector fields V_i , \vec{R}_i and A_i are zero. Hence one gets the following radial equations for the meson and Coulomb fields

$$\left(-\frac{1}{r} \frac{d^2}{dr^2} \cdot r + U'(\sigma) \right) \sigma(r) = - \sum_B g_{\sigma B} \rho_{s,B}(r) \quad (36)$$

$$\left(-\frac{1}{r} \frac{d^2}{dr^2} \cdot r + m_\omega^2 \right) V_0(r) = \sum_B g_{\omega B} \rho_{v,B}(r) \quad (37)$$

$$\left(-\frac{1}{r} \frac{d^2}{dr^2} \cdot r + m_\rho^2 \right) R_{0,0}(r) = \sum_B g_{\rho B} \tau_{0,B} \rho_{\text{iso},B}(r) \quad (38)$$

$$-\frac{1}{r} \frac{d^2}{dr^2} (r \cdot A_0(r)) = \sum_B q_B e \rho_{v,B}(r) \quad (39)$$

where the scalar, vector, and isovector densities are given by the sum over the occupied single particle wave functions

$$\rho_{s,B}(r) = \bar{\Psi}_B \Psi_B = \sum_{\alpha=1}^N \omega_{\alpha,B} \varphi_{\alpha,B}^+(r) \gamma_0 \varphi_{\alpha,B}(r) \quad (40)$$

$$\rho_{v,B}(r) = \bar{\Psi}_B \gamma_0 \Psi_B = \sum_{\alpha=1}^N \omega_{\alpha,B} \varphi_{\alpha,B}^+(r) \varphi_{\alpha,B}(r) \quad (41)$$

$$\rho_{\text{iso},B}(r) = \bar{\Psi}_B \gamma_0 \tau_{0,B} \Psi_B = \sum_{\alpha=1}^N \omega_{\alpha,B} \varphi_{\alpha,B}^+(r) \tau_{0,B} \varphi_{\alpha,B}(r) \quad (42)$$

with the occupation number $\omega_{\alpha,B}$ for each baryon species and $\tau_{0,B}$ stands for the isospin of the baryon. The wavefunctions for the baryons can be separated into upper and lower components by the ansatz

$$\varphi_{\alpha,B}(r) = \begin{pmatrix} \frac{iG_{\alpha,B}(r)}{r} & Y_{j_\alpha l_\alpha m_\alpha} \\ \frac{F_{\alpha,B}(r)}{r} \frac{\sigma \cdot r}{r} & Y_{j_\alpha l_\alpha m_\alpha} \end{pmatrix} \quad (43)$$

with the spherical harmonics Y_{jlm} and the normalization

$$\int_0^\infty \{ |G_{\alpha,B}(r)|^2 + |F_{\alpha,B}(r)|^2 \} dr = 1 \quad . \quad (44)$$

The Dirac equations can then be written in terms of these two components

$$\varepsilon_{\alpha,B} G_{\alpha,B}(r) = \left(-\frac{d}{dr} + \frac{\kappa_{\alpha,B}}{r} \right) F_{\alpha,B}(r) \quad (45)$$

$$+ (m_B + g_{\sigma B} \sigma(r) + g_{\omega B} V_0(r) + g_{\rho B} \tau_{0,B} R_{0,0}(r) + q_B e A_0(r)) G_{\alpha,B}(r)$$

and

$$\begin{aligned} \varepsilon_{\alpha,B} F_{\alpha,B}(r) &= \left(+ \frac{d}{dr} + \frac{\kappa_{\alpha,B}}{r} \right) G_{\alpha,B}(r) \\ &- (m_B + g_{\sigma B} \sigma(r) - g_{\omega B} V_0(r) - g_{\rho B} \tau_{0,B} R_{0,0}(r) - q_B e A_0(r)) F_{\alpha,B}(r) \end{aligned} \quad (46)$$

with

$$\kappa_{\alpha,B} = \begin{cases} -(j_{\alpha} + \frac{1}{2}), & j_{\alpha} = l_{\alpha} + \frac{1}{2} \\ +(j_{\alpha} + \frac{1}{2}), & j_{\alpha} = l_{\alpha} - \frac{1}{2} \end{cases} \quad (47)$$

The densities can be rewritten to

$$\rho_{s,B}(r) = \frac{1}{4\pi r^2} \sum_{\alpha=1}^N \omega_{\alpha,B} (2j_{\alpha} + 1) [G_{\alpha,B}(r)^2 - F_{\alpha,B}(r)^2] \quad (48)$$

$$\rho_{v,B}(r) = \frac{1}{4\pi r^2} \sum_{\alpha=1}^N \omega_{\alpha,B} (2j_{\alpha} + 1) [G_{\alpha,B}(r)^2 + F_{\alpha,B}(r)^2] \quad (49)$$

$$\rho_{\text{iso},B}(r) = \frac{1}{4\pi r^2} \sum_{\alpha=1}^N \omega_{\alpha,B} (2j_{\alpha} + 1) \tau_{0,B} [G_{\alpha,B}(r)^2 + F_{\alpha,B}(r)^2] \quad . \quad (50)$$

The occupation numbers are

$$\omega_{\alpha} = \begin{cases} +1 \\ -1 \end{cases} \quad (51)$$

for closed shells. Otherwise one chooses the occupation number in the interval $0 < \omega_{\alpha,B} < 1$ according to a schematic pairing

$$\omega_{\alpha,B} = \frac{1}{2} \left[1 - \frac{\varepsilon_{\alpha,B} - \varepsilon_{\text{Fermi},B}}{\sqrt{(\varepsilon_{\alpha,B} - \varepsilon_{\text{Fermi},B})^2 + \Delta^2}} \right] \quad (52)$$

analogous to Skyrme-Hartree-Fock calculations [59] where

$$\Delta = \frac{11.2 \text{ MeV}}{\sqrt{A}} \quad (53)$$

is a constant gap derived from nuclear pairing properties. The Fermi-energy $\varepsilon_{\text{Fermi},B}$ is evaluated in such a way, that the baryon number is conserved for each species.

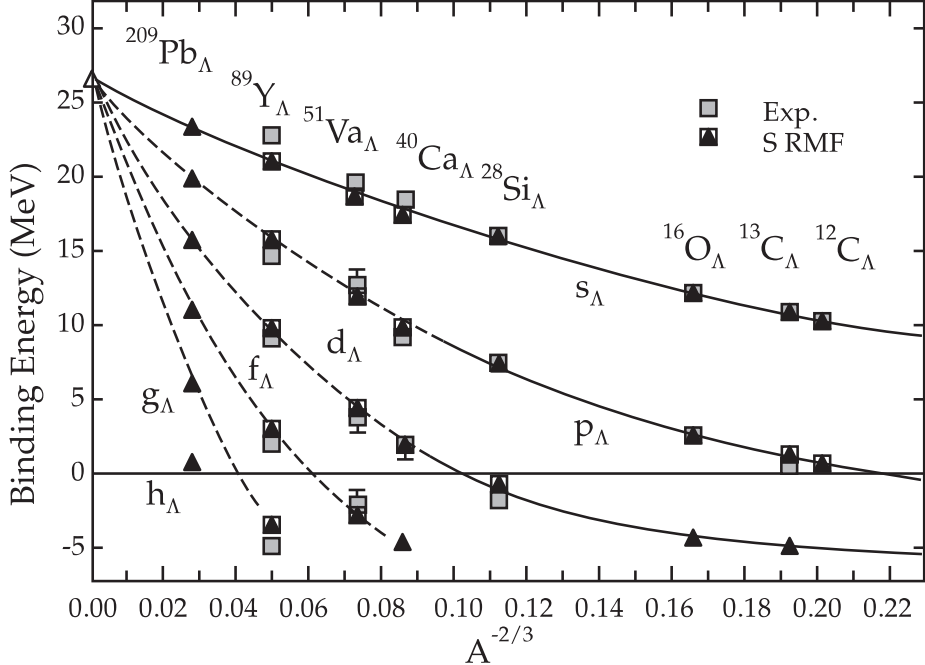


Fig. 8. The single particle energy of several hypernuclei in comparison with RMF calculations.

The coupled equations (36)-(39) and (45),(46) together with the above expressions for the densities can be solved iteratively using standard techniques (for details see [60]). The parameters of the model are fitted to the properties of spherical nuclei [61,60] where we will use the stabilized parameter set PL-Z [58] in the following. The RMF model gives a description of nuclei as good as the conventional Skyrme-Hartree-Fock calculations [55]. Also the binding energy of hypernuclei can be nicely reproduced (see [37–39], for fits to recent hypernuclear data see [41,42]).

Fig. 8 shows the measured single particle energy for different hypernuclei in comparison with RMF calculations. One sees nicely the different single particle levels of the Λ . Note that the spin-orbit splitting for Λ levels is negligible therefore the shells can be labeled by s-shell, p-shell and so on. Bulk matter ($A \rightarrow \infty$) corresponds to the crossing of the energy levels with the y-axis. All levels merge to the value of the Λ potential depth in nuclear matter of about 27 MeV.

It turns out that the two coupling constants of the Λ ($g_{\sigma\Lambda}$ and $g_{\omega\Lambda}$) are strongly correlated because they are fixed by the potential depth of the Λ

$$U_\Lambda = -g_{\sigma\Lambda}\sigma - g_{\omega\Lambda}V_0 \quad (54)$$

in saturated nuclear matter [62]. Hence one can choose for example SU(6)-symmetry for the vector coupling constants (see table 4) and fixes the scalar

coupling constants to the potential depth of the corresponding hyperon.

Nevertheless, this model, hereafter named model 1, is not able to reproduce the observed strongly attractive $\Lambda\Lambda$ interaction as can be seen in fig. 9 irrespectively of the chosen vector coupling constant. Model 1 does not give the necessary strong attraction between the two Λ 's. An additional interaction has to be invoked between hyperons. This can be done by using a SU(3) symmetric model and introducing two additional meson fields, the scalar meson $f_0(975)$ (denoted as σ^* in the following) and the vector meson $\phi(1020)$ [63,48] which we will discuss in the following.

3.4 Hyperon-Hyperon interactions

The additional Lagrangian for the new mesons is straight forward to derive

$$\mathbf{L}' = \mathbf{L} + \mathbf{L}_{\text{Meson}}^{YY} + \mathbf{L}_{\text{Coupling}}^{YY} \quad (55)$$

with

$$\mathbf{L}_{\text{Meson}}^{YY} = \frac{1}{2} \left(\partial_\nu \sigma^* \partial^\nu \sigma^* - m_{\sigma^*}^2 \sigma^{*2} \right) - \frac{1}{4} S_{\mu\nu} S^{\mu\nu} + \frac{1}{2} m_\phi^2 \phi_\mu \phi^\mu \quad (56)$$

$$\mathbf{L}_{\text{Coupling}}^{YY} = - \sum_B g_{\sigma^* B} \bar{\Psi}_B \Psi_B \sigma^* - \sum_B g_{\phi B} \bar{\Psi}_B \gamma_\mu \Psi_B \phi^\mu \quad (57)$$

and the notation

$$S_{\mu\nu} = \partial_\mu \phi_\nu - \partial_\nu \phi_\mu \quad . \quad (58)$$

The new meson fields give new potential terms for the Dirac equations

$$\begin{aligned} \varepsilon_{\alpha,B} \varphi_{\alpha,B}(r) = & \gamma_0 \left\{ -i \vec{\gamma} \cdot \vec{\nabla} + m_B + g_{\sigma B} \sigma(r) + g_{\sigma^* B} \sigma^*(r) \right. \\ & \left. + g_{\omega B} \gamma^0 V_0(r) + g_{\phi B} \gamma^0 \phi_0(r) + g_{\rho B} \gamma^0 R_{0,0}(r) + q_B e \gamma^0 A_0(r) \right\} \varphi_{\alpha,B}(r) \end{aligned} \quad (59)$$

and two new meson field equations

$$(-\Delta + m_{\sigma^*}^2) \sigma^*(r) = - \sum_B g_{\sigma^* B} \rho_{s,B}(r) \quad (60)$$

$$(-\Delta + m_\phi^2) \phi_0(r) = \sum_B g_{\phi B} \rho_{v,B}(r) \quad (61)$$

g_{MB}	Nucleon	Λ	Σ	Ξ
ω	3	2	2	1
ρ	1	0	2	1
ϕ	0	$-\sqrt{2}$	$-\sqrt{2}$	$-2\sqrt{2}$

Table 4

The vector coupling constants in SU(6)-symmetry relative to $g_{NN\rho}$.

which are written here in the static RMF approximation.

The vector coupling constants to the ϕ -field are given by SU(6)-symmetry (see table 4). How does one get these relations?

Here we discuss the coupling scheme for the baryons to mesons in SU(3) symmetry. The baryons are members of an octet, the mesons of a nonet (a octet plus a singlet) under SU(3) symmetry. Coupling two octets (for example two baryons) results in

$$8 \otimes 8 = 1 \oplus 8^1 \oplus 8^2 \oplus 10 \oplus 10^* \oplus 27 . \quad (62)$$

These terms have to be multiplied with the octet of the mesons now and the result must be an overall singlet, so that the interaction (and the Lagrangian) is invariant under SU(3) symmetry. As there appears two octets in the above product, there are two possibilities to form an overall singlet in the Lagrangian. They are usually called symmetric and antisymmetric coupling. The latter one is given by

$$\mathbf{L}_f = -g_8 \cdot i f_{imn} \bar{\psi}_m \psi_n \phi_i , \quad (63)$$

with the antisymmetric structure constants of SU(3)

$$f_{imn} = \frac{1}{4i} \text{Tr}([\lambda_m, \lambda_n] \lambda_i) \quad (64)$$

and therefore also called F-type coupling. The octet coupling constant g_8 is a universal coupling strength. One can rewrite the structure of the above interaction in matrix form. We normalize the SU(3) matrices as

$$\text{Tr} \lambda_i \lambda_j = 2\delta_{ij} . \quad (65)$$

and define the baryon and meson matrices as

$$\bar{B} = \frac{1}{\sqrt{2}} \lambda_m \bar{\psi}_m \quad B = \frac{1}{\sqrt{2}} \lambda_n \psi_n \quad M = \lambda_i \bar{\phi}_i \quad (66)$$

This gives the compact notation

$$\mathbf{L}_f = -g_8 \cdot \text{Tr}([\bar{B}, B]M) \quad (67)$$

The case for the symmetric coupling is analogous. Here the symmetric structure constants defined as

$$d_{imn} = \frac{1}{4} \text{Tr}(\{\lambda_m, \lambda_n\} \lambda_i) \quad (68)$$

give

$$\mathbf{L}_d = -g_8 \cdot d_{imn} \bar{\psi}_m \psi_n \phi_i = -g_8 \cdot \text{Tr}(\{\bar{B}, B\}M) \quad . \quad (69)$$

This is also called the D-type coupling.

The baryon matrix is given explicitly as

$$B = \begin{pmatrix} \frac{1}{\sqrt{2}}\Sigma^0 + \frac{1}{\sqrt{6}}\Lambda^0 & \Sigma^+ & p \\ \Sigma^- & -\frac{1}{\sqrt{2}}\Sigma^0 + \frac{1}{\sqrt{6}}\Lambda^0 & n \\ -\Xi^- & \Xi^0 & -\frac{2}{\sqrt{6}}\Lambda^0 \end{pmatrix} \quad , \quad (70)$$

and analogous for the antibaryon matrix. The general form of the Yukawa coupling is a mixture of D-type and F-type coupling

$$\mathbf{L}_{\text{SU}(3)} = -g_8 \alpha \text{Tr}([\bar{B}, B]M) + g_8(1 - \alpha) \text{Tr}(\{\bar{B}, B\}M) \quad . \quad (71)$$

Here α denotes the F/(F+D) ratio. For the vector mesons one gets the following coupling terms

$$\begin{aligned} \mathbf{L}_{\text{SU}(3)} = & -g_{NN\rho} \bar{N} \tau N \rho - g_{\Sigma\Lambda\rho} (\bar{\Sigma} \Lambda + \bar{\Lambda} \Sigma) \rho - g_{\Sigma\Sigma\rho} \bar{\Sigma} \tau \Sigma \rho - g_{\Xi\Xi\rho} \bar{\Xi} \tau \Xi \rho \\ & - g_{NN\omega_8} \bar{N} N \omega_8 - g_{\Lambda\Lambda\omega_8} \bar{\Lambda} \Lambda \omega_8 - g_{\Sigma\Sigma\omega_8} \bar{\Sigma} \Sigma \omega_8 - g_{\Xi\Xi\omega_8} \bar{\Xi} \Xi \omega_8 \\ & - g_{\Lambda N K^*} (\bar{N} \tau \Lambda K^* + \bar{\Lambda} \tau N \bar{K}^*) - g_{\Sigma N K^*} (\bar{N} \tau \Sigma K^* + \bar{\Sigma} \tau N \bar{K}^*) \\ & - g_{\Xi \Lambda K^*} (\bar{\Lambda} \tau \Xi K^* + \bar{\Xi} \tau \Lambda \bar{K}^*) - g_{\Xi \Sigma K^*} (\bar{\Sigma} \tau \Xi K^* + \bar{\Xi} \tau \Sigma \bar{K}^*) \end{aligned} \quad (72)$$

and the meson-baryon coupling constants are now related to the F/(F+D) ratio and the overall octet coupling strength by

$$\begin{aligned}
g_{NN\rho} &= g_8 & g_{\Sigma\Lambda\rho} &= \frac{2}{\sqrt{3}}g_8(1 - \alpha_{ps}) & g_{\Sigma\Sigma\rho} &= 2g\alpha_{ps} \\
g_{NN\omega_8} &= \frac{1}{\sqrt{3}}g_8(4\alpha_{ps} - 1) & g_{\Lambda\Lambda\omega_8} &= -\frac{2}{\sqrt{3}}g_8(1 - \alpha_{ps}) & g_{\Sigma\Sigma\omega_8} &= \frac{2}{\sqrt{3}}g_8(1 - \alpha_{ps}) \\
g_{\Xi\Xi\omega_8} &= -\frac{1}{\sqrt{3}}g_8(1 + 2\alpha_{ps}) & g_{\Lambda NK^*} &= -\frac{1}{\sqrt{3}}g_8(1 + 2\alpha_{ps}) & g_{\Sigma NK^*} &= g(1 - 2\alpha_{ps}) \\
g_{\Xi\Lambda K^*} &= \frac{1}{\sqrt{3}}g_8(4\alpha_{ps} - 1) & g_{\Xi\Sigma K^*} &= -g_8 & g_{\Xi\Xi\rho} &= -g(1 - 2\alpha_{ps}).
\end{aligned}$$

As noted before, there is also a singlet state for the mesons which couples to all baryons with the same strength

$$\mathbf{L}_1 = -g_1(\bar{N}N + \bar{\Lambda}\Lambda + \bar{\Sigma}\Sigma + \bar{\Xi}\Xi)\omega_1 \quad , \quad (73)$$

which means that

$$g_{NN\omega_1} = g_{\Lambda\Lambda\omega_1} = g_{\Sigma\Sigma\omega_1} = g_{\Xi\Xi\omega_1} \quad . \quad (74)$$

The physical states are not ω_8 and ω_1 but the ω meson and the ϕ meson which are mixed states

$$\begin{aligned}
\omega &= \omega_8 \cos \theta - \omega_1 \sin \theta \\
\phi &= \omega_8 \sin \theta + \omega_1 \cos \theta \quad .
\end{aligned} \quad (75)$$

For the vector meson it is known, that the ϕ meson is nearly a pure $s\bar{s}$ state as it decays mainly to kaons. Under this condition, the mixing is called ideal and the mixing angle is $\tan \theta = 1/\sqrt{2}$, $\theta \approx 35.3^\circ$.

If the nucleon does not couple to the (purely strange) ϕ meson, then

$$g_1 = \sqrt{6}g_8 = \sqrt{6}g_{NN\rho} \quad . \quad (76)$$

In SU(6) symmetry, which is a special case of SU(3) symmetry, only the F-type coupling remains for the vector mesons. This is in accordance with the vector dominance model [64]. In this case, the relations for the vector mesons can be given as in table 4. These relations reflect simple quark counting rules. So the Λ couples to the ω meson only $2/3$ as strong as the nucleon, as it has only two light quarks. On the other side, the doubly strange baryon Ξ couples twice as strong to the (hidden) strange meson ϕ compared to the Λ which has only one strange quark.

The scalar coupling constants to the σ^* -field are fixed by the potentials

$$U_{\Xi}^{(\Xi)} \approx U_{\Lambda}^{(\Xi)} \approx 2U_{\Xi}^{(\Lambda)} \approx 2U_{\Lambda}^{(\Lambda)} \approx 40 \text{ MeV} \quad (77)$$

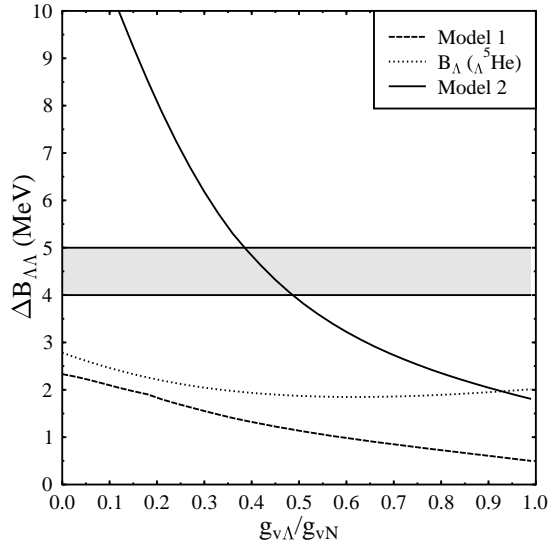


Fig. 9. The matrix element $\Delta B_{\Lambda\Lambda}$ as a function of the vector coupling constant in model 1 and 2.

which is motivated from one-boson exchange models and the measured strong $\Lambda\Lambda$ interaction [48]. Note that the nucleons do not couple to these new fields. This fixes all the parameters of model 2.

This extended model 2 is now closer to the experimental value of the $\Lambda\Lambda$ interaction matrix element (see fig. 9). Due to the additional attractive forces coming from the hidden strange meson exchange, the $\Lambda\Lambda$ matrix element is now much stronger than in model 1.

3.5 Properties of Strange Hadronic Matter

In the following we study the properties of metastable exotic multihypernuclear objects (MEMO's). Metastability means that strong processes are forbidden, so that the system can only decay weakly and lives therefore on the timescale of the weak interaction of 10^{-10} s. Inside a bound system some of the strong processes can be energetically forbidden due to medium effects, i.e. the strong reaction is Pauli-blocked. Only two processes



have such low Q-values that this effect occurs in a bound system.

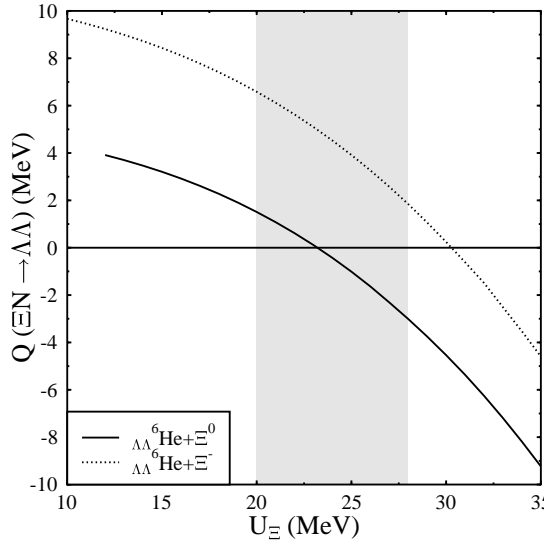


Fig. 10. The Q-value of the strong process $\Lambda\Lambda \rightarrow \Xi N$ for the system with $A = 7$ and $S = -4$ as a function of the potential depth of the Ξ in nuclear matter. The process is not allowed for negative values, hence the system can only decay weakly.

Therefore we study systems composed of $\{p, n, \Lambda, \Xi^0, \Xi^- \}$ and search for metastable combinations by the following recipe:

- Start with a deeply bound nuclear core, e.g. ${}^4\text{He}$ or ${}^{56}\text{Ni}$, so that the neighboring nuclei are much less bound.
- Fill up the Λ -levels so that the products of the above reactions are Pauli-blocked.
- Add as many Ξ 's as possible unless the strong reactions can open.

The effect of the Pauli-blocking is demonstrated in Fig. 10 for the lightest possible system ${}_{\Xi^0\Lambda\Lambda}{}^7\text{He}$. The Q-value is given by

$$Q = m_\Xi + m_N - 2m_\Lambda - B_\Xi(1s) - B_N(1s) \quad (80)$$

and is plotted versus the potential depth of the Ξ in nuclear matter. The system is likely to be bound and metastable if this value gets negative. This happens for $U_\Xi > 22$ MeV which is in accordance with experiment.

Heavier systems with a doubly magic nucleon core like ${}^{208}\text{Pb}$ can be also filled up with hyperons (Λ , Ξ^0 , and Ξ^-) selfconsistently so that they are metastable according to the recipe outlined. The presence of many hyperons will change the sequence of single-particle energies and accordingly the magic numbers appreciably. One gets a new shell ordering for a large strangeness $|S|$. Fig.

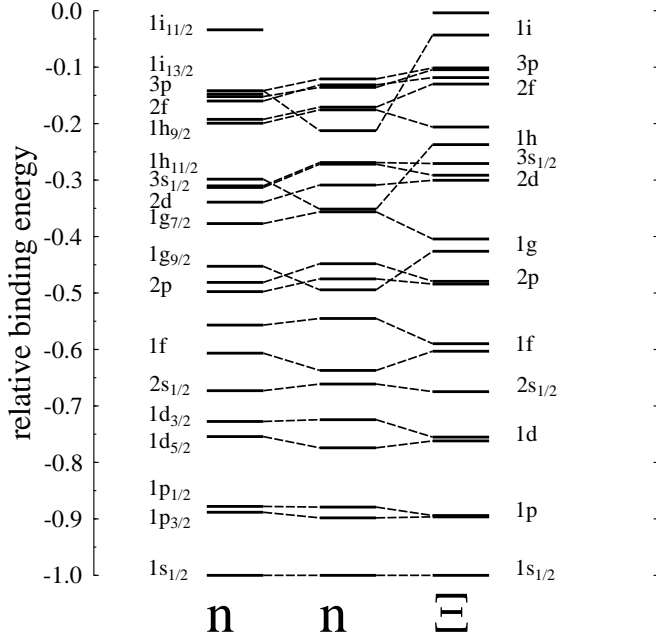


Fig. 11. The single particle energy of the system ^{208}Pb with 70Λ , $18 \Xi^0$, and $70 \Xi^-$ (middle column: neutron levels, right column: Ξ^0 levels). The neutron levels for ^{208}Pb are shown in the left column for comparison.

11 shows the single particle energies of the system ^{208}Pb with 70Λ , $18 \Xi^0$, and $70 \Xi^-$ which is bound by $E_B/A = -12.9$ MeV. The neutron levels in the ordinary nucleus (left column) and in the strangeness-rich system (middle column) are compared to each other. The shell levels show some reordering especially for the higher lying levels due to the presence of many hyperons. For the protons, the change is more pronounced due to Coulomb effects and the magic number is now 70. The single particle levels of the Ξ^0 indicates a quite small spin-orbit splitting. They are heavier than nucleons and in addition feel a smaller spin-orbit force than nucleons due to the smaller coupling constants. The magic numbers here are the ones of the Wood-Saxon potential without spin-orbit splitting: 2, 8, 18, 20, 34, 58, and 92.

The density distribution of the system with hyperons is plotted in Fig. 12. The density distribution for the nucleons is still around normal nuclear density. The total density is increased to about $2\rho_0$ as the hyperon density has to be added up. Note, that the hyperons are treated as distinguishable point particles. Effects which take into account the substructure of the hadrons might alter this picture but will be not discussed here. The Λ density distributions shows a broad surface as the Λ single particle levels are occupied until the least bound level which ensures the Pauli blocking mechanism for the Ξ 's. The Ξ^- 's are less bound than the protons so that the charge density changes sign at the surface and gets negative.

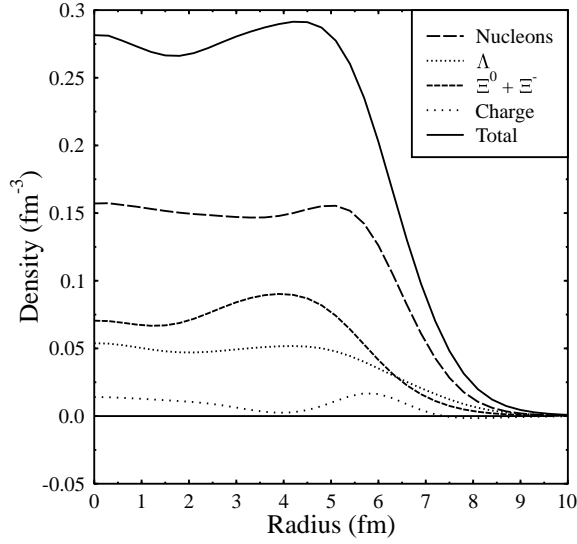


Fig. 12. The density distribution of the system ^{208}Pb with 70 Λ , 18 Ξ^0 , and 70 Ξ^- .

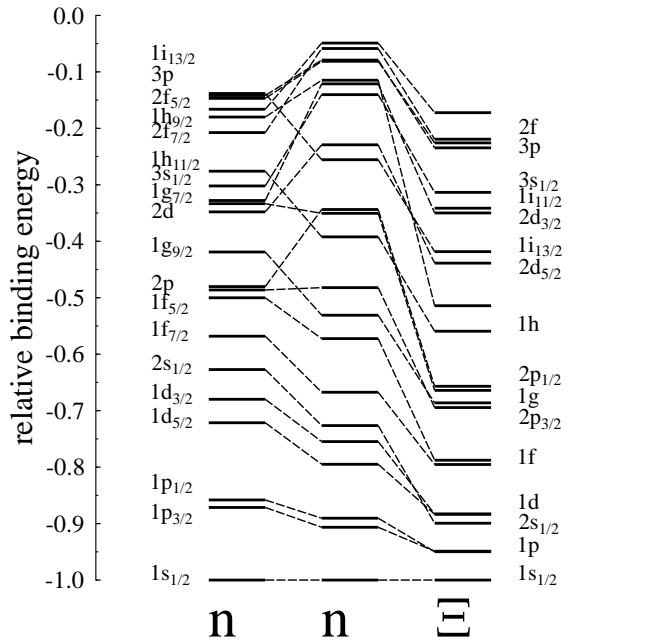


Fig. 13. The single particle energy of the system ^{180}Th with 92 Λ , 92 Ξ^0 , and 70 Ξ^- (middle column: neutron levels, right column: Ξ^0 levels). The neutron levels for ^{180}Th are shown in the left column for comparison.

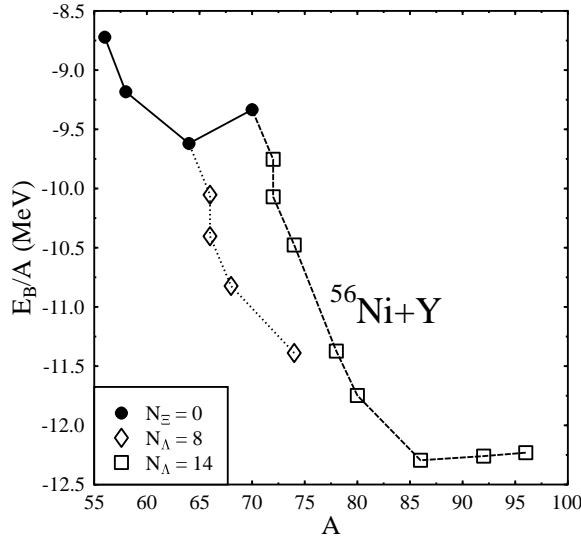


Fig. 14. The binding energy per baryon versus the baryon number A for ^{56}Ni with hyperons added in model 1.

An analogous example for model 2 with the strongly attractive hyperon-hyperon interaction is the system ^{180}Th with 92 Λ , 92 Ξ^0 , and 70 Ξ^- . Now the binding energy is $E_B/A = -21.4$ MeV emerging from the additional attractive forces between the hyperons. The nucleus ^{180}Th itself is unstable and emits protons immediately. The presence of the hyperons, especially the negatively charged Ξ^- 's, shift the unbound proton levels down, so that all the proton levels are bound. The magic numbers for nucleons has changed then from 82 to 90 for both, neutrons and protons for large $|S|$. The big level changes can be seen in Fig. 13. In particular, the $n = 1$ (nodeless) levels are more bound than in ordinary nuclei. Also for the Ξ levels, the nodeless 1i level now appears below the 3s level contrary to the ordinary oscillator shell ordering.

Now we discuss the calculations for several sequences starting with a nuclear core and subsequently filling up the levels with hyperons. Fig. 14 shows the case for the nuclear core ^{56}Ni in model 1. When the p-shell of the Λ 's is filled ($N_\Lambda = 8$) it is energetically favourable to add Ξ 's to the system. If the next shell is also filled up ($N_\Lambda = 14$), the maximum number of added Ξ 's can be even higher enriching the system with a lot of strangeness.

Fig. 15 shows the sequences for the doubly magic cores ^{56}Ni , ^{132}Sn , ^{208}Pb , and ^{310}G ($Z = 126$, $N = 184$). The glue-like effect of the hyperons result in an enhanced binding energy. Adding hyperons stabilizes the systems, i.e. enhances the binding energy due to the opening of a new degree of freedom. Mass numbers of $A \approx 500$ can be easily reached with a rather large binding

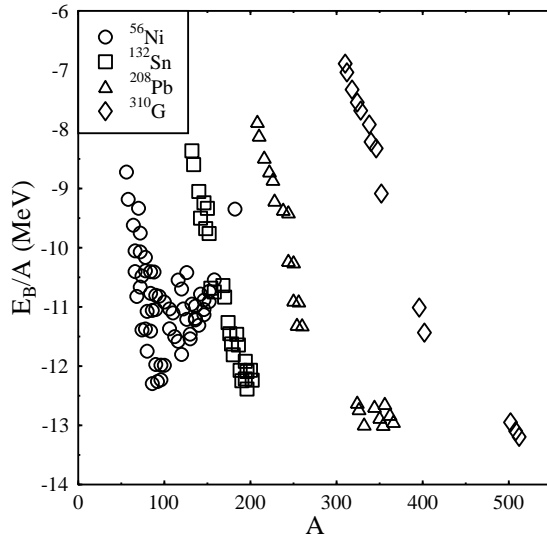


Fig. 15. The binding energy per baryon in model 1 for various sequences starting with ^{56}Ni , ^{132}Sn , ^{208}Pb and the superheavy nuclear core ^{310}G with 126 protons and 184 neutrons.

energy of $E_B/A \approx -13$ MeV. These systems are stabilized due to the presence of the Ξ^- , which avoid the instability due to the Coulomb repulsion. The Pb sequence has systems with a total charge of $Z = 12$ (82 protons and 70 Ξ^-). For the Ni sequence, one gets also zero charged systems with 28 protons and 28 Ξ^- . Adding further hyperons for the small systems results in less binding, therefore the parabolic shape for the Ni sequence. One sees a linear shape for the heavier cores by adding more and more hyperons. The sequences of the heavier systems stop when the Λ levels are filled up and this happens before there are more Ξ^- 's than protons so that one sees only a linear curve.

The analogous sequences for model 2 are depicted in Fig. 16 for the nuclear cores ^{56}Ni and ^{180}Th . The other cores (^{132}Sn , ^{208}Pb , and ^{310}G) are not doubly magic anymore for large $|S|$. The system ^{180}Th is considerably stabilized with a large injection of hyperons. About 150 hyperons are needed to achieve stability. The region of stability extends from $A = 330$ to $A = 578$.

Purely hyperonic systems, composites of $\{\Lambda, \Xi^0, \Xi^-\}$ only, are stable in model 2 up to $A \approx 200$. They are denoted as Y which should not be confused with the ordinary Ytterbium nucleus. Typical binding energies are $E_B/A = -5$ to -8.5 MeV. The most stable system is the one for $A = 60$ with 14 Λ , 28 Ξ^0 , and 18 Ξ^- . The Coulomb repulsion prevents systems larger than $A \approx 200$. Interestingly, hyperonic matter is always highly negatively charged. These systems are lying between $-0.5 < Z/A < -0.2$. Moreover, the strangeness fraction is

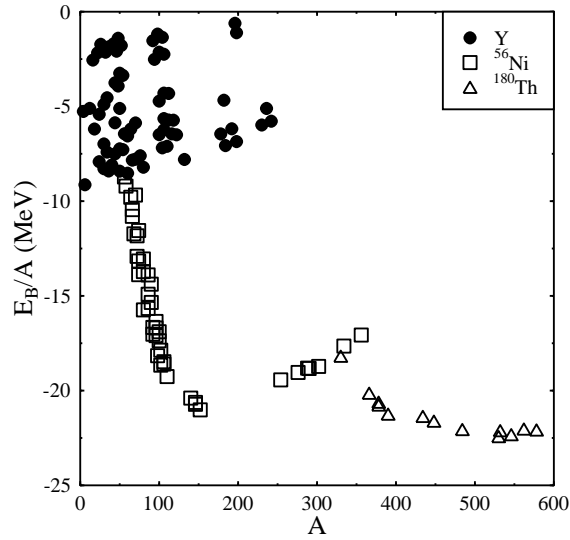


Fig. 16. The binding energy per baryon in model 2 for various sequences starting with ^{56}Ni , and ^{180}Th . The symbol Y denotes purely hyperonic systems.

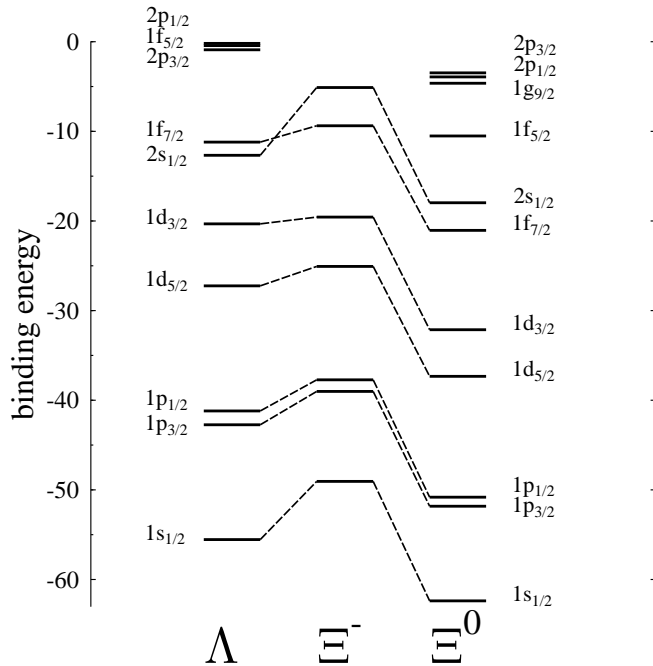


Fig. 17. The single particle energy of the purely hyperonic system $\{18\Lambda, 34\Xi^0, 28\Xi^-\}$ in model 2.

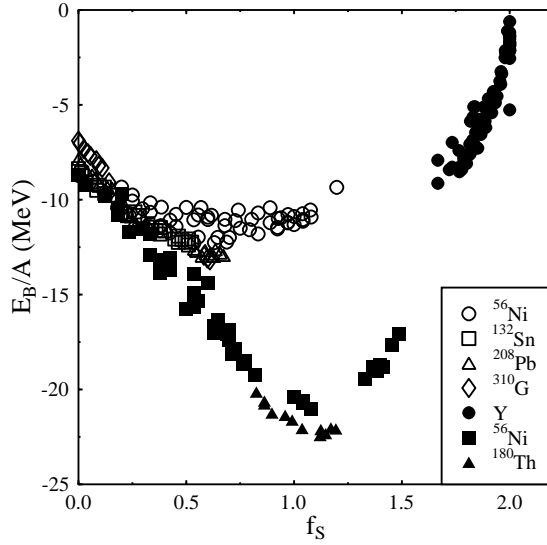


Fig. 18. Binding energy versus the strangeness fraction for SHM in model 1 (nuclear cores ^{56}Ni , ^{132}Sn , ^{208}Pb , ^{310}G) and model 2 (^{56}Ni , ^{180}Th , Y denotes purely hyperonic systems).

also very high $f_s > 1.6$ for this type of matter. For isospin saturated systems of $\{\Lambda, \Xi^0, \Xi^-\}$ one gets the values $f_s = 5/3$ and $Z/A = -1/3$, respectively. The lightest bound system is likely to be $\{2\Lambda, 2\Xi^0, 2\Xi^-\}$ where every hyperon fills up their respective 1s-shell. Fig. 17 shows as an example the single particle energy for the hyperonic system $\{18\Lambda, 34\Xi^0, 28\Xi^-\}$. The 1s-state has a binding energy between 50 and 60 MeV for all three hyperon species. This reflects more or less the assumed universal hyperon-hyperon interaction. The energy levels of the Ξ^0 are a little bit deeper than the ones of the Λ due to the higher mass. The Coulomb repulsion shifts the states of the Ξ^- to smaller binding energy compared to the others.

The binding energy of strange hadronic matter is plotted in Fig. 18 versus the strangeness fraction $f_s = |S|/A$ for both models for various nuclear cores. It is interesting to note that the minima of the curves are located around $f_s \approx 0.6$ for model 1 and $f_s \approx 1.0$ for model 2 which is in the same range as for strangelets. The minima found in Fig. 18 correspond to charge to mass ratios around zero very similar to the property of strange quark matter in its groundstate. Nevertheless, the main difference between strangelets and strange hadronic matter, except, of course, of their internal structure, is that the maximum binding energy of $E_B/A \approx -13$ MeV (model 1) and $E_B/A \approx -23$ MeV (model 2) is by far to less to overcome the mass difference between nucleons and hyperons of about 177 MeV. Strange hadronic matter will thus decay weakly on a timescale comparable to the lifetime of a Λ -hyperon.

4 STRANGE MATTER IN RELATIVISTIC HEAVY ION COLLISIONS

Collision experiments of heavy ions at high bombarding energies may be the only unrevealing chance and opportunity for both the production and detection of small pieces of strange quark matter: One major goal of these experiments is to unfold the temporary creation and existence of the quark gluon plasma phase. A direct proof of this fleetingly small moment turns out to be a difficult and complicated task. One therefore has to find signals which come directly and only from the transient existence of the QGP. This will be different, if a (meta-)stable strange quark droplet will show up during the break-up. This is quite similar to the situation in the early universe [11], where a remnant (or ‘ash’) of the QGP is created. In fact, it seems rather selfevident that a deconfined quark matter state could probably act as a good starting point for the agglomeration of quarks to strangelets, because the quarks are thought to move quasifreely over longer distances similar as in the situation inside strange quark matter.

In this section, we review the ideas that had led to the search for strangelets at present heavy ion experiments at Brookhaven and at CERN: In the first subsection, the important mechanism of strangeness separation in the phase transition of a quark gluon plasma back to hadronic degrees of freedom will be explained [3]. The second subsection then addresses the exciting possibility of producing strange quark matter droplets in heavy ion collisions. In particular we will discuss why such droplets might cool and form long-lived cold strangelets. In the last subsection we will close our discussion in critically emphasizing the detection possibilities of strangelets and small MEMOs by their properties and lifetimes, also in respect to the present experimental undertaking at Brookhaven and at CERN.

4.1 *Strangeness separation during the QGP phase transition*

In nuclear collisions, strangeness can only be produced in $s\bar{s}$ pairs due to the conservation of hypercharge in strong interactions. Thus, at first sight, there seems to be no chance to really succeed for producing strangelets: The net strangeness of the plasma state counting the difference of strange to antistrange quarks is zero from the onset of the fireball’s expansion. In this subsection we want to give arguments, that first if a *baryon-rich* and hot QGP is created in such collisions and second if the strangeness degree of freedom is nearly saturated, the strange quarks will separate from the antistrange quarks in a nearly equilibrium deconfinement \leftrightarrow confinement transition and will predominantly remain in the plasma phase [3].

According to fluid dynamic or microscopic models baryon stopping, (baryon-)dense and hot matter formation and partial thermalization has to be expected at AGS and CERN energies for central collisions and heavy systems [65]. One should be aware of the fact, that the energy and baryon densities reached are so large, that a phase transition to a quark gluon plasma may have occurred.

It was suggested and shown already some time ago that an abundant number of strange and antistrange quarks are produced in a hot QGP [66] by gluon fusion and that, accordingly, strangeness saturates the phase space after a very short equilibration time which may actually be shorter than the lifetime of the QGP phase [6,67]. In the meantime, an enhancement of strange particle production in nuclear collisions has been observed in many experiments [68–71]. However, it has also been learned that such an enhancement alone does not make a reliable signature for the QGP. Strange particles, especially K mesons and Λ hyperons can be copiously produced in hadronic reactions before the nuclear fireball reaches equilibrium [72]. Yet, the enhancement of the Λ hyperon over a wider rapidity range [71] and especially the observed and strongly enhanced yields of antihyperons [69–71], which were also proposed as a signature for QGP [6], require particular microscopic modifications of the hadronic cascades: Color rope formation [73]; multiple string breaking and (!) decaying multi-quark droplets [74]. Such modifications can already be considered as precursor phenomena associated with QGP formation.

In the following, the deconfinement phase transition is assumed to be of first order, implying that the relaxation times for chemical transmutations as well as the hadronization time are small compared to the overall transition time. The Gibbs criteria read

$$\begin{aligned} T_{QGP} &= T_{HG} , \\ P_{QGP} &= P_{HG} , \\ \mu_{QGP}^B &= \mu_{HG}^B , \\ \mu_{QGP}^s &= \mu_{HG}^s . \end{aligned} \tag{81}$$

In particular the last condition is significant for the separation to be discussed: In a Gibbs phase equilibrium the chemical potentials are continuous across the phase boundary, whereas the corresponding densities are (or might be) discontinuous. This first implies that the abundance of especially the strange hadrons during the equilibrium transition are governed by the same quark-chemical potentials, μ_q for the light quarks and μ_s for the strange quarks, e.g.

$$\begin{aligned} \mu_{K,\bar{K}} &= \pm \mu_q \mp \mu_s , \\ \mu_{\Lambda,\bar{\Lambda}} &= \pm 2\mu_q \pm \mu_s , \end{aligned}$$

$$\begin{aligned}\mu_{\Xi, \bar{\Xi}} &= \pm \mu_q \pm 2\mu_s , \\ \mu_{s, \bar{s}} &= \pm \mu_s .\end{aligned}\tag{82}$$

Second, the corresponding density to the strange quark potential is the net strangeness content, i.e. the strangeness ratio f_s defined in (3). In general this ratios need *not* to be the same during transition: $f_s^{QGP}(\mu_q, \mu_s, T) \neq f_s^{HG}(\mu_q, \mu_s, T)$.

Fig. 19. Schematic picture of the separation of strangeness during phase transition in a baryon-rich system

Consider now the phase transition of the QGP to the hadron gas at some critical temperature. *How does the strange and antistrange quarks hadronize during this transition?* There is no stringent reason why these different quarks do hadronize in the same manner and time, especially if one thinks of a baryon rich system. At the beginning of the hadronization ($t = t_S$) there is only the QGP phase. Because of an overall strangeness conservation the number of strange quarks equals the number of antistrange quarks, the strange chemical potential $\mu_s = 0$ and the net strangeness content of the plasma phase is that of the system, $f_s^{QGP}(t = t_S) \equiv 0$. Now, quarks combine to hadronic particles and leave the plasma phase, but hadrons may also decompose and go back to the plasma state. Because of the progressing expansion of the whole fireball, however, the hadron phase turns bigger while the plasma phase decreases. It is ‘simple’ for the antistrange quarks to materialize into kaons, because of the (immense) surplus of massless quarks compared to their antiquarks. The strange quarks can combine to Λ -particles, but these are rather heavy and it is energetically much easier for them to stay in the plasma, when hadronization proceeds. The possible strangeness content in the two different phases is schematically drawn in Fig. 19. A large antistrangeness builds up in the hadron matter while the QGP retains a large net strangeness excess. This separation will occur only when the system carries a positive net baryon number.

Fig. 20. Fraction of net strangeness to baryon number present in the QGP phase as a function of the baryochemical potential μ_q and the volume fraction χ . Note that f_s can exceed 0.5. The path of an isentropic expansion is also shown.

To be more specific, requiring that the total strangeness during the phase transition in the combined system of two phases vanishes, leads to the constraint

$$V_{QGP}(\rho_s - \rho_{\bar{s}}) + V_{HG}(\rho_K + \rho_Y - \rho_{\bar{K}} - \rho_{\bar{Y}}) \equiv 0 . \quad (83)$$

Together with the Gibbs criteria of pressure equilibrium, (81), the phase transition temperature and the strange quark potential are then implicit functions of the quark chemical potential μ_q , and, for example, the volume fraction χ of the hadron phase to the total system, i.e. $\chi = V^{HG}/(V^{HG} + V^{QGP})$ [3]. In Fig. 20 the fraction $f_s^{QGP}(\mu_q, \mu_s, T)$ of strange quarks to all quarks present in the QGP is shown as a function of the quark potential μ_q and the volume fraction χ . At the beginning of the phase transition ($V^{HG} = 0$) the well known result $\mu_s = 0$ is recovered, s and \bar{s} quarks are produced in pairs only. On the other hand, for vanishing QGP ($V^{QGP} = 0$) zero net strangeness leads to a nonzero value of the strange chemical potential $\mu_s > 0$ [3]. A different strange particle production shows up in the dominance of the associated production over the direct pair production at finite baryon density. During the coexistence of the two phases, an additional channel opens up for the strangeness: besides the associated pair production in the hadron gas it is possible to have, for example, associated production of a K - meson in the sector of the hadron gas phase and the s-quark staying in the QGP. This leads to a net strangeness content $f_s^{QGP}(t > t_S)$ larger than 0 in the quark phase and to a diminished hyperon abundance, $f_s^{HG} < 0$, the hyperons being too massive, in the hadronic gas sector at finite net baryon densities. At vanishing overall net baryon density, i.e.

at $\mu_q = 0$, (and vanishing net strangeness density) the transition is completely symmetric for strange and antistrange particles, i.e. $\mu_s = 0$ throughout the transition, and separation can not occur as one would expect.

Of special importance is the fact that the accumulation of s quarks in the plasma phase grows with decreasing plasma volume. This opens up the possibility that s-quarks may be bound not only in hyperons and strange mesons: They could form strange quark matter clusters or MEMOs which might be metastable objects. A baryon-rich environment may thus be more feasible for strangelets than the situation in the hot quark phase in the early universe with only a tiny small surplus. Also the cooling of the plasma should in addition not only be due to the expansion, but also due to ‘prefreezeout’ evaporation processes of hadronic particles, because of the relatively small length scale in heavy ion collisions compared to the astrophysical picture: Surface processes like evaporation should become important. This issue and the possible distillation of strangelets will be discussed in the next subsection.

Finally we remark that the separation mechanism can be probed by density interferometry with hyperons [75] or kaons [76]. The hadrons with negative strangeness, the Λ , \bar{K} and \bar{K}^0 , are expected to be produced mainly at the last stage of the phase transition when the size of the quark phase volume has become quite small. As the hyperons or antikaons are quite heavy, their thermal velocity is relatively small so that at freeze-out they probably still will be localized near the center of the system. Such a close localization $r_0 \approx 2 - 3$ fm can be seen by measuring two particle correlations with the Hanbury-Brown-Twiss method. In Fig. 21 the pair correlation function of two Λ particles is shown under the assumption that a rather strong possible resonance channel contributes at low momenta. This might occur because of a possible strong attractive Λ - Λ -interaction (see section 3). Especially with such a channel small source sizes are relatively clean to determine. (Of course, the observation of such a resonance would give some exciting new *experimental* insight on the interaction among two Λ s.) If the separation does not occur or if there is no QGP the deduced source size should be nearly the same as for kaons or pions and thus considerably larger.

4.2 Strangelet distillation

Besides the onset of strangeness separation during the equilibrium phase transition there exist another, somehow related argument which could lead to strangelet formation in ultrarelativistic heavy ion collisions [4,77]. Rapid kaon emission from the ‘surface’ (or, in other words, the outer region) of the fireball can result in an even stronger enhancement of the s-quark abundance in the quark phase. As important, this prompt kaon (and, of course, pion) emission

Fig. 21. The pair correlation function of emitted Λ hyperons is shown for different source sizes under the assumption of a relatively strong resonance channel.

may in addition cool the quark phase, so that there really might be a chance that the quark plasma droplet condenses into metastable or stable, rather cold droplets of strange quark matter [4].

In order to model the evolution of an initially hot fireball a two phase *equilibrium* description between the hadron gas and the QGP was combined with the *nonequilibrium* radiation by incorporating the rapid freeze-out of hadrons from the hadron phase surrounding the QGP droplet during the phase transition [5]. In particular we will then address the question whether, how and why a hot QGP droplet can cool and will then form (or better ‘become’) a long-lived cold lump of strange quark matter. Before we turn to the model we summarize the reasoning for the existence and the possible consequences of the evaporation processes.

Let us make some crude estimates about the qualitative features of the surface radiation of a *baryon-rich* fireball. One first might think of meson radiation off the initial pure quark phase by various microscopic processes [77–80]. The most dominant particles to be evaporated are the pions. For the strange mesons the K^+ , K^0 are more easily radiated in a baryon-rich environment off the hot surface of the quark phase than K^- and \bar{K}^0 [4]. Similarly and probably even more important should be the meson radiation while the system is in the phase coexistence region. On one hand most of the total collision time is spent in this region On the other hand, the possibility of reabsorption of mesons is very unlikely, since the system approaches freeze-out. Meson evaporation in both stages of the expansion just described carries away entropy, energy *and*

antistrangeness. Therefore, the residual expanding fireball, which is in the mixed phase, loses entropy and is charged up with a net strangeness larger than zero. For a rough estimate a thermal black-body-type radiation formula can be employed. Accordingly the emission of $\bar{K}s$ containing an \bar{q} -quark are then suppressed from baryon-rich matter by a factor $\sim e^{-2\mu_q/T}$ as compared to the Ks . Adding the resulting numbers over the different stages of the fireball, a loss in entropy per baryon of about 15 units [4] and a net strangeness enrichment of the total system of about $f_s^{total} = 0.75$ is found [77,4]! The assumption of black body radiation seems intuitively plausible from detailed balance arguments [81] if one thinks that each hadron moving towards the ‘surface’ of the plasma phase will first coalescence and then be completely absorbed.

The mechanism by which a QGP state is converted into hadrons is a major uncertainty in the different descriptions. The hadronization transition has often been described by geometric and statistical models, where the matter is assumed to be in partial or complete equilibrium during the whole expansion phase. A hydrodynamic expansion is often assumed, which is substantially modified by the phase transition [82,67]. Partial departure from (strange) chemical equilibrium is allowed in the flavour kinetic model [6,67,83]. These rate calculations suggested that chemical equilibrium is reached in the hadron phase, if the system evolves from the deconfined phase: gluon fusion yields fast equilibration of strangeness. The subsequent re-hadronization affects that the strange hadron yields closely approach the hadron equilibrium yields *from above*.

A more realistic scenario must take into account the competition of the collective expansion with the particle radiation from the surface of the hadronic fireball before ‘freeze out’. In a second class of models [84,85] it is assumed that the plasma breaks up into droplets at some point during the hadronization transition. In a ‘cascade’ model [85] the emission and reabsorption of pions from the surface of the hot plasma was studied. For the present purpose, evaporation of other hadrons must also be taken into account. Nucleons and strange particles (e.g. kaons and hyperons) are particularly important. One important outcome of the cascade model [85] was the observation that the total entropy is approximately constant during the hadronization.

Our following model [5] combines in a simple, yet plausible way the two different classes. The expansion of the QGP droplet during the phase transition will be described within a two-phase equilibrium; in particular the strangeness degree of freedom is thought to stay in chemical equilibrium because the complete hadronic particle production is driven by the plasma phase, as suggested by the rate calculations. The competition of the collective expansion with the particle radiation is incorporated by rapid freeze-out of hadrons from the outer layer of the hadron phase surrounding the QGP droplet at the Gibbs phase transition point. The expansion is here assumed to be quasiisentropic,

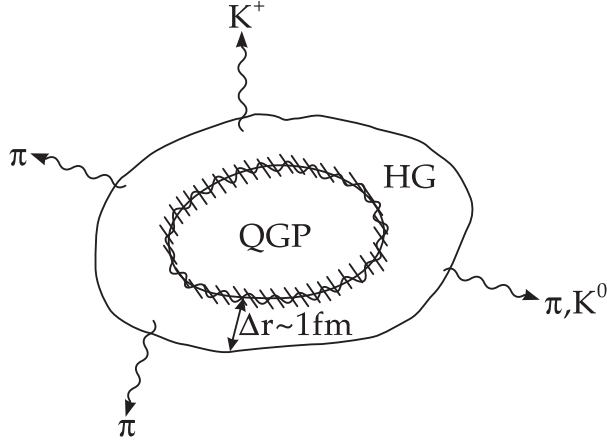


Fig. 22. Hadron fluid surrounds the QGP at the phase transition. Particles evaporate from the hadronic region. New hadrons emerge out of the plasma by hadronization.

as suggested by the cascade model. This scenario is visualized in Fig. 22.

The global properties of the two phase system then change in time in accord with the following differential equations for the baryon number, the entropy and the net strangeness number of the total system:

$$\begin{aligned}
 \frac{d}{dt} A^{tot} &= -\Gamma A^{HG} \\
 \frac{d}{dt} S^{tot} &= -\Gamma S^{HG} \\
 \frac{d}{dt} (N_s - N_{\bar{s}})^{tot} &= -\Gamma (N_s - N_{\bar{s}})^{HG} ,
 \end{aligned} \tag{84}$$

where $\Gamma = \frac{1}{A^{HG}} \left(\frac{\Delta A^{HG}}{\Delta t} \right)_{ev}$ is the effective ('unique') rate of particle (of *converted hadron gas volume*) evaporated from the hadron phase. These three equations may easily be combined in a physically illustrative form:

$$\begin{aligned}
 \frac{d}{dt} \left(\frac{S}{A} \right)^{tot} &= -\Gamma \lambda^{HG} (1 - \lambda^{HG}) \left(\left(\frac{S}{A} \right)^{HG} - \left(\frac{S}{A} \right)^{QGP} \right) \\
 \frac{d}{dt} f_s^{tot} &= -\Gamma \lambda^{HG} (1 - \lambda^{HG}) (f_s^{HG} - f_s^{QGP}) ,
 \end{aligned} \tag{85}$$

where $\lambda^{HG} = 1 - \lambda^{QGP} = A^{HG}/A^{tot}$ is the ratio of baryon number contained in the hadron phase over the total baryon number in the system, f_s defines the total net strangeness content of the system, and $\frac{S}{A}$ is the entropy per baryon. The three equations (84,85) constitute a set of *coupled* differential equations

for A^{tot} , $(S/A)^{tot}$ and f_s^{tot} . The latter two are given in terms of the hadron and quark phase content by

$$\left(\frac{S}{A}\right)^{tot} = \left(\frac{S}{A}\right)^{QGP}(\mu_q, \mu_s, T)(1 - \lambda^{HG}) + \left(\frac{S}{A}\right)^{HG}(\mu_q, \mu_s, T)\lambda^{HG} \quad (86)$$

$$f_s^{tot} = f_s^{QGP}(\mu_q, \mu_s, T)(1 - \lambda^{HG}) + f_s^{HG}(\mu_q, \mu_s, T)\lambda^{HG} .$$

The equation of state used consists of the Bag-model for the QGP and a mixture of relativistic Bose-Einstein and Fermi-Dirac gases of the well established nonstrange and strange hadrons up to $M \sim 2$ GeV for the hadron matter.

Although the baryon number A and the strangeness f_s are conserved under strong interactions, their value in the system changes with time according to the above equations due to the evaporation process. This calculation requires solving simultaneously the equations of motion and the Gibbs phase equilibrium conditions (81), which specify the intrinsic variables (e.g. the chemical potentials) of the functions $\left(\frac{S}{A}\right)^{QGP/Had}(\mu_q, \mu_s, T)$ and $f_s^{QGP/Had}(\mu_q, \mu_s, T)$. Still the effective rate Γ and the baryon fraction λ^{HG} are not specified. Intuitively, the plasma is surrounded by the hadron phase, thus we take it as a shell of constant thickness of $\Delta r \sim 1$ fm (this is an ad hoc assumption, however, as it turns out, the results depend only weakly on this thickness). This then specifies λ^{HG} . Some unique hadron gas volume of the outer layer is then evaporated in a small time interval Δt . For the unknown evaporation time we use an averaged rate of all particles at the considered temperature, dictating the time-scale for the evolution of the hadronic particles out of the hadron phase. Altogether, the quasiadiabatic expansion during hadronization and the evaporation of the hadrons in the most outer regions are both incorporated and dictate the evolution of the (plasma) droplet and its intrinsic variables μ_q, μ_s and T .

For the following arguments it is important to study the expansion of an initially hot QGP fireball with special attention to the evolution of the strangeness during the phase transition. As outlined above, early non-equilibrium particle radiation off the pure hot and dense (baryon-rich) QGP fireball is expected to be important in the initial phase of the reaction. Pions and kaons (containing an \bar{s} -quark) (and only a minor number of antikaons) are emitted from the surface of the plasma. Thus the QGP is enriched with finite net strangeness even *before* the phase transition point is reached. The net strangeness enrichment resulting from the early black body radiation off the pure QGP-droplet has been estimated to be in the range $f_s^{init} \lesssim 0.5$ [77,4]. These values have been used in the present model as input for the initial condition $f_s(t_0)$ when hadronization starts. In a complete isentropic expansion with a total (initial) net strangeness content but *without* further particle evaporation it was (al-

ready) shown [4,86] that for not so high initial entropies the evolution can end with a small and (meta-)stable strangelet, if the employed QGP equation of state will allow for such exotic configurations to exist at small temperatures. We will see in the following how things will work.

Fig. 23. (a) Baryon number, strangeness content and temperature of the quark glob during complete hadronization as a function of time for a very large bag constant $B^{\frac{1}{4}} = 235$ MeV. The initial values are an initial baryon content of $A_B(t_0) = 100$, an entropy per baryon ratio of $\frac{S}{A}(t_0) = 25$ and an initial net strangeness fraction of $f_s(t_0) = 0.25$. Note the strong increase of the strangeness content with time. (b) The same situation as in (a), however, for a small bag constant $B^{\frac{1}{4}} = 145$ MeV, when a strangelet is *distilled*. One observes a strong decrease in the evolving temperature.

Fig. 23 gives an impression how the hadronization proceeds for a large bag

constant ($B^{1/4} = 235$ MeV – no strangelet in the groundstate) and a small bag constant ($B^{1/4} = 145$ MeV). The initial parameters are a small net strangeness content of $f_s(t_0) = 0.25$ and a moderate entropy per baryon ratio of $\frac{S}{A}(t_0) = 25$ (which is expected at CERN SPS energies): For the large bag constant the system hadronizes completely in $t \sim 8 \frac{fm}{c}$, which is customarily expected and thus not surprising. The quark droplet remains unstable until the strange quarks have clustered into Λ -particles and other strange hadrons to carry away the strangeness and the plasma has completely vanished into standard particles. Yet, a strong increase of the net strangeness of the system is found in both situations, which is basically a confirmation of the strangeness separation mechanism and will be analyzed in some more detail below. The plasma drop reaches a strangeness fraction of $f_s \gtrsim 1.5$ when the volume becomes small. Indeed, for the *small* bag constant, however, a cold strangelet emerges from the expansion and evaporation process with an approximate baryon number of $A \sim 22$, a radius of $R \sim 2.5 fm$, and a net strangeness fraction of $f_s \gtrsim 1.5$, i.e. a charge to baryon ratio $Z/A \sim -0.25$! This would be an interesting object also from its global properties: It would comprise a nucleus of positive baryon number, but negative charge.

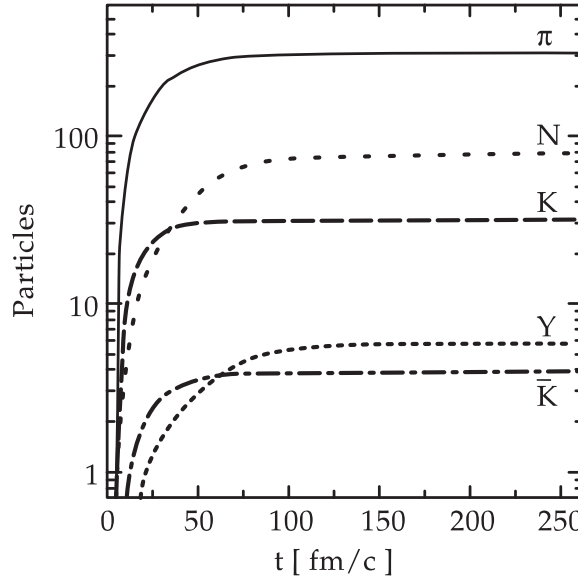


Fig. 24. The number of emitted particles are shown versus time in a situation, when a strangelet is distilled. The conditions are the same as in Fig. 23, however, no initial net strangeness is assumed.

The particle yields of the most frequently emitted species are shown in Fig. 24 for the case, where a strangelet condenses after $\sim 100 \frac{fm}{c}$, although the total net strangeness was zero at the beginning of the hadronization. Their time dependence is more or less as expected: Roughly 300 pions and 32 kaons are produced prior to most of the other hadron species, followed by the nucleons (~ 77) and at the late stage by some antikaons (~ 3) and hyperons (~ 6). The total K^+/π^+ -ratio is then approximately 0.16. The surplus of 17 in baryon

number and of 23 in strangeness are contained in the missing strangelet, which has to have a strangeness fraction of $\sim 1.4!$ The temporal behavior of the emitted particles underlines the important role played by the kaons (and pions) during hadronization. The early leaving kaons do enrich the remaining system with net strangeness. The pions carry about half of the available entropy off the system. For this reason one might expect that the nonequilibrium aspects can become even more efficient at still higher entropies, when more kaons and pions are produced.

One observes that in both cases depicted in Fig. 23 the net strangeness increases. However, in the first case, at high critical temperatures, the temperature of the system increases slightly, although one might have expected some cooling by the emission of particles, whereas in second case, strangelet formation goes hand in hand with strong cooling. As a compelling consequence the temperature (and entropy) decreases drastically throughout the hadronization and condensation process. Thus the pressure goes to zero and an absolutely stable, cold strangelet is created. The energy per baryon of the remaining strange quark droplet converges to its zero temperature value.

Why does in both (model) cases the net strangeness content increase? Consider therefore the physical content of eqs. (85). Obviously, Γ , λ^{HG} and $(1 - \lambda^{HG})$ are larger than zero. Therefore, the total net strangeness fraction f_s^{tot} of the system will always increase or decrease, respectively, with time, if the fraction f_s^{HG} is smaller or larger, respectively, than f_s^{QGP} . Of course, this is just the question whether or not the separation of strangeness does occur. The abundant presence of the kaons enforces $f_s^{HG} < 0$ early on! Also later on f_s^{HG} remains smaller than f_s^{QGP} , and therefore f_s^{tot} increases as function of time ($\frac{d}{dt} f_s^{tot} > 0$).

Why is there cooling in the one and reheating in the other case? Here a rather similar argument holds for the total entropy. The total entropy of the remaining system $(S/A)^{tot}$ will decrease ($\frac{d}{dt}(S/A)^{tot} < 0$), i.e. the system will be cooled, if and only if the specific entropy per baryon in the hadron phase exceeds that in the quark phase, $(S/A)^{HG} > (S/A)^{QGP}$. The system will reheat, i.e. $(S/A)^{tot}$ will increase ($\frac{d}{dt}(S/A)^{tot} > 0$), if and only if $(S/A)^{HG} < (S/A)^{QGP}$. It was pointed out already in ref. [4] that the strangelet formation can only go hand in hand with strong *cooling* rather than reheating. This is the case when the bag constant $B^{\frac{1}{4}}$ is small and allows for the existence of (meta-)stable strange quark matter states. Although this intimate connection between cooling of the plasma phase and the existence of strange quark matter is intriguing, it might be valid only within the simple parametrization of the quark gluon plasma phase within a bag model description. Ultimately, whether $(S/A)^{HG}$ is larger or smaller than $(S/A)^{QGP}$ at finite, nonvanishing chemical potentials might theoretically only be proven rigorously by lattice gauge calculations in the future, as also the principle existence of (meta-)stable strange quark

matter.

In the situation when a strangelet gets distilled out of the original QGP phase, one observes [5] that the values of the two chemical potentials approach ‘rather’ quickly their asymptotic numbers, even when the temperature of the strangelet is still not so small, $T \sim 40 - 60$ MeV: or metastable):

- $\mu_q \sim 200 - 275$ MeV , $\mu_s \sim 300 - 325$ MeV ($B^{\frac{1}{4}} = 145$ MeV);
- $\mu_q \sim 200 - 250$ MeV , $\mu_s \sim 350 - 400$ MeV ($B^{\frac{1}{4}} = 160$ MeV).

The evaporation of the particles forces these potentials to become quasistationary; a detailed balance for the emission of nucleons and *antikaons* has adjusted itself. The hyperon emission is still strongly suppressed compared to the nucleons, although the strange chemical potential is already larger than the light quark potential. (For higher bag parameters, the hyperons become more and more important. It is exactly when strangelets are getting barely stable to unstable when the hyperon emission becomes as or even more efficient in the late stages of the plasma phase than the one for the nucleons.) A ‘simple’ but basic idea for the possible formation of strange quark matter droplets is due to behavior of the nucleons. As discussed in the section 2, the total energy per baryon (at finite temperature this has to be substituted by the free energy) can easily be lowered by assembling the non-strange quarks into pure nucleonic degrees of freedom as long as the strangelet is not at its minimum value in f_s . This happens rather fast. For finite temperatures the surplus in thermal energy provides additional nucleon evaporation, so that this minimum point will be ‘overshot’ and the strangelet turns out to have a strangeness fraction larger than 1. To further illustrate how then stable strangelets cool and survive, we note first that with the above numbers an effective nucleon binding energy $I_n = m_n - 3\mu_q \sim 120 - 350$ MeV is found in the late stages of the process. The energy per baryon of a strangelet at small temperature and zero pressure is approximately given by

$$\frac{E}{A} = \left(\frac{E}{A} \right)_{T=0} + \gamma T^2 , \quad \gamma \sim \frac{1}{20} \frac{1}{MeV} \quad (87)$$

Any late emission of a nucleon will now decrease the energy per baryon of the blob:

$$\Delta \left(\frac{E}{A} \right) = \frac{I_n}{A(T)} \Delta A , \quad \Delta A < 0 .$$

In addition, the differential of eq. (87) is $\Delta(E/A) = 2\gamma T \Delta T$. Combining these two simplified expressions and integrating from the initial temperature T_i to $T = 0$ yields roughly the final baryon number of the strangelet:

$$A^{final} = A(T_i) \exp \left(\frac{-\gamma T_i^2}{I_n} \right) . \quad (88)$$

For $I_n \sim 250$ MeV and $T_i \sim 20$ MeV, a total of ~ 92 percent of the initial baryon number would remain in the droplet. Hence, evaporation of baryons from quark matter will be suppressed at very low temperatures (and will cool the droplet), because there is simply not enough thermal energy available to power the complete evaporation. The strangelet becomes cold and stable.

We have so far demonstrated that under certain circumstances, the hadronization can result in the distillation of a rather cold strange quark matter droplet. This debris of the quark gluon plasma can, of course, only survive, if the energy per baryon of the strange quark object is smaller than the energy per baryon of the corresponding hadronic system at the same f_s . For the bag model the strangelet is stable for $B^{\frac{1}{4}} = 145$ MeV or metastable for $B^{\frac{1}{4}} = 160 - 180$ MeV. For realistic parameters modeling the initial situation of the QGP fireball either in the stable or metastable situation one might expect a reasonable strangelet with a baryon number $\sim 10 - 30$ [5]. Negatively charged strangelets result for all cases calculated in [5]:

- $f_s(t \rightarrow ' \infty ') \sim 1.1 - 1.5$, $Z/A \sim (-0.05) - (-0.25)$ – stable case ;
- $f_s(t \rightarrow ' \infty ') \sim 1.5 - 2.0$, $Z/A \sim (-0.25) - (-0.5)$ – metastable case .

One should emphasize the fact that the charge of the distilled strangelet (with positive baryon number) is found to be negative! This seems counterintuitive as the most stable configurations should actually be, though small, positively charged. This has to do with the final nucleon emission which is still energetically possible if the strangelet carries still a positive charge. Its charge then can only be changed by weak processes. (Please note our previous discussion above. We will come back to this point also in the next section when we address the important question of what are the most likeliest candidates to be seen in the dedicated experiments.)

As long as finite size effects like surface tension or curvature contributions are neglected, the equations of motion (84) are scale invariant. All extensive properties, the rate Γ and the time t do scale for example with the initial baryon content $A_B(t_0)$. Thus, in order to distill a strangelet with a baryon number much larger than 1, the initial quark gluon plasma droplet must be fairly large. (Not only) for this reason the heavy ion experiments using the heaviest ions, like the available Au- and Pb-beams, should be most favourable for strangelet search.

The distillery works even for larger initial entropies $S/A=50$ or 100 [5,87]. A high initial entropy does not necessarily prohibit strangelet formation. Abundant kaon production enriches the plasma rapidly with net strangeness at high entropies. This might offer to look for strangelet production at the highest bombarding energies available in the present and future for very heavy

systems, e.g. at the CERN SPS ($E_{LAB} \sim 200 \frac{GeV}{N}$) or even at RHIC ($E_{LAB} \sim 20 \frac{TeV}{N}$) facilities. One might even think that the distillation indeed could also work for very small initial chemical potentials, i.e. $\mu_q/T \ll 1$, as will be expected in the central rapidity region at RHIC energies (although there still might be a noticeable, nonvanishing net baryon excess) and LHC energies [87]. There might be fluctuations at some, but no particular rapidity region where a small but net excess in baryon number as well as in strangeness number statistically occurs. Within the present model this can lead to a distillation of very small strangelets of a size $A_B \leq 5$ [87]. There is a lot of wishful thinking in this scenario, as it assumes that at the onset of the transition the system is in chemical equilibrium and due to the fluctuations is described by very small, but finite chemical potentials. It is amusing to note some analogy with the cosmological scenario proposed by Witten [11]. The tiny net baryon excess in the early universe hiding in the ‘high-temperature’ phase is tremendously small, even compared to the numbers expected at the LHC energies due to fluctuations. The distillation of strange quark matter Witten visualizes as a shrinking, leaking ‘balloon’, where only neutrinos are allowed to escape, leaving the net baryon density back and trapped inside the balloon. This picture assumes neutrino losses are the main way for the high-temperature phase to lose energy and baryon diffusion to be negligible, while in fact neutrino losses and surface evaporation might appear comparable. In the present case the mesons take the part of the neutrinos and it is the question how efficient their emission is compared to the evaporation of baryons, so that a cooling really might take place.

We conclude that there are two essential processes which can favour the formation of strangelets from a baryon-rich QGP formed in ultrarelativistic heavy ion collisions. The first (as a prerequisite) is the s - \bar{s} -separation mechanism discussed in the section before. This leaves us with a quark phase in the coexistence region of hadronic and quark matter, which is charged up with strangeness. The s -quarks, created in pairs with \bar{s} -quarks in the early quark-gluon fireball, remain in the quark phase during the phase transition, the \bar{s} -quarks materialize mainly into kaons. The second is the evaporation of the hadronic gas with its antistrangeness excess, which charges the remaining system with net strangeness. Besides the expansion additional pion and nucleon evaporation should help to allow for a possible, yet necessary cooling. All these processes are statistical in nature. These calculations are strictly valid only for large systems. Large fluctuations around these average predictions have to be expected, in particular for the strangeness production per event and for the evaporation processes. In a real heavy ion collision an idealized situation as put forward in the present description is probably never reached. The results here should be seen with this in mind. They should illustrate that if (meta-)stable strangelets do (or can) exist in nature, there might really be a chance for their production at the present and future relativistic heavy ion experiments.

4.3 Detectability in heavy ion experiments

An important prediction of the exploited model in the previous subsection is the *negative* charge to mass ratio, $Z/A \sim -0.1$ for absolutely stable strangelets, and $Z/A \sim -0.45$ for metastable droplets. Still, not restricting too much to this model, the produced strangelets or MEMOs might also be slightly positive [4]. It then could be detected by its unusual charge-to-mass ratio ($\sim +0.15 < Z/A < -0.5$).

On the other hand, simple coalescence estimates give production probabilities of strange clusters of the order of $10^{3-A_B-|S|}$, where S denotes the strangeness and A_B the baryon number of the cluster [9,88]. Small clusters with $A_B + |S| \leq r + 3$, where r is the sensitivity of the apparatus (presently $r \leq 12$), are most favoured for detection. Therefore, if strangelets or MEMOs are formed due to this scenario, baryon numbers of $A_B \leq 12$ are expected.

It is important to note that these objects are a *new form of matter*, not a specific new particle. The strange droplets produced in these reactions do not come in the form of a single type of particle. Many different sizes of droplets may be produced, spanning a range in mass, charge, and strangeness content. The experimental task of finding the new form of matter is therefore challenging. Here any detected particle having an unusual charge to mass ratio is a potential *hypermatter* candidate.

To identify a particle or cluster, its charge and mass need to be measured. To determine that the particle is a new form of strange matter, its strangeness content must also be revealed. The experimental approach is first to find ‘objects’ having a peculiar or new charge/mass ratio. (The strangeness might be seen by interaction with a secondary nucleus : multiple production of Λ s, Σ s, Ξ s and \bar{K} s in such a secondary reaction would signal its existence.) The key idea here is that the charge/mass ratio will be unlike that of any normal nuclear isotope (the 8He with a $Z/A = 0.25$ would be the isotope candidate with the smallest ratio). Strangelets (or MEMOs) would have a charge ~ 0 , being slightly positively or negatively charged. In particular in the range $-0.25 < Z/A < +0.25$ there exists no quasistable form of nuclei or antinuclei. Such a range will has been covered by the E864[89] experiment at Brookhaven. E878, the successor of E858[90], using a focusing spectrometer at zero degree, is seizing a much smaller selected range, which in respect to cover still the full range of interest can be steadily adjusted. A similar technique like in E878 is also been employed by the Newmass collaboration[91] (NA52 experiment) at CERN at much higher energies, and at the present time also with the heavy Pb -beam.

The question remains, on which time-scale weak decay or flavour changing

modes will appear. How would a strangelet or MEMO then look like when passing through the detector? Employing TOF-techniques to reveal the velocity and thus the charge to mass ratio, the experimental setup sets a natural time scale $\sim 10^{-8}$ sec. So, an important question we finally have to address are the lifetimes of these objects. In the following, we subsequently discuss the properties of both forms of strange matter and the possible long- and short-lived candidates referring to [92].

Whether or not strangelets exist depends crucially on the value of the bag constant which is not known for such strange and big systems. For a bag constant of $B^{1/4} = 145$ MeV, the original value of the MIT bag model fit, strangelets are absolutely stable, for bag constants up to $B^{1/4} \approx 180$ MeV strangelets are metastable, i.e. they can decay by weak interactions. So anything between absolutely stable and unbound is possible. Nevertheless, for the following arguments one needs only three basic assumptions:

- (1) Strange quark matter is at least metastable.
- (2) There exists a local minimum for the total energy per baryon of strange quark matter at a finite strangeness fraction $f_s = |S|/A$.
- (3) The relativistic shell model can be used for strangelets.

With these assumptions we demonstrate that there exists a valley of stability at low mass numbers and that these strangelets are highly negatively charged contrary to former findings.

The MIT bag model is used here as a guideline only. Fig. 25 shows the energy per baryon number of isospin symmetric strangelets as a function of f_s for $A \leq 40$ for a bag parameter of $B^{1/4} = 170$ MeV. Now there are three different processes which will shift a strangelet emerging from a heavy ion collisions to a very high strangeness fraction. First, the strangelets sitting above the line drawn between the nucleon and the hyperon masses will decay to a mixture of nucleons and hyperons by strong interactions completely as this is energetically favored. Second, the strangelets located between that line and the tangent construction starting at the nucleon mass (denoted as strong) can still decay *strongly* on a timescale of 10^{-20} sec by emitting nucleons and hyperons. They will be shifted to a higher strangeness fraction until they reach the tangent point at $f_s \approx 1.4$ (confer our discussion at the end of the previous subsection). Third, weak nucleon decay can occur for the strangelets between the former tangent and the other tangent (denoted as weak) starting at the nucleon mass and $f_s = 1$ (as weak interaction change one unit of strangeness) [9]. The timescale for a weak nucleon decay has been estimated to lie between 10^{-7} – 10^{-9} sec [93]. More conservatively, one could also argue that it might be comparable to that of a Λ -particle. For a strangelet with $f_s > 1$ the weak

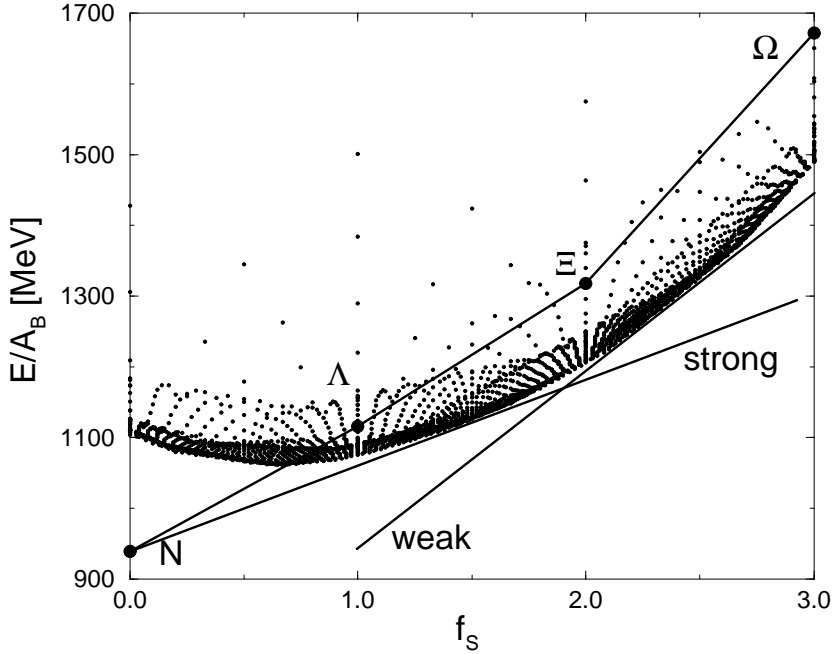


Fig. 25. The energy per baryon E/A_B of isospin symmetric strangelets with $A_B \leq 40$ for a bag constant of $B^{1/4} = 170$ MeV versus the strangeness fraction f_s . The solid line connects the masses of nucleon, Λ , Ξ and Ω and stands for free baryon matter.

nucleon decay will enhance the strangeness fraction as

$$\Delta f_s = \frac{|S| - 1}{A - 1} - \frac{|S|}{A} = \frac{f_s - 1}{A - 1} . \quad (89)$$

Hence, strangelets surviving strong and weak nucleon decay (and which thus can be detected with present experimental setups) can be sitting at a very high strangeness fraction of $f_s \approx 2.2$ which is the weak tangent point in Fig. 25. For isospin symmetric systems, this large strangeness fraction corresponds to a charge fraction of

$$\frac{Z}{A} = \frac{1}{2} (1 - f_s) = -0.55 \quad (90)$$

which indicates highly charged strange quark matter. This is contrary to the conventional picture that strangelets have a slightly positive charge-to-mass ratio which is the case for strange matter sitting in the minimum of the curve plotted in Fig. 25. But as pointed out before, the combined effect of strong and weak hadronic decay will shift strangelets emerging from a heavy ion collision to much higher values of f_s and therefore to highly negatively charged objects!

This simplified picture is only valid in bulk matter. For finite systems, which we are interested in, shell effects will be important (see already our discussion in section 2). Already in Fig. 25 one sees that shell effects are at the order of 100 MeV per baryon number! Hence, we expect that strangelets with a closed shell can be very deeply bound. These 'magic' strangelets are most likely to be stable against strong and weak hadronic decay modes as their decay products have a much higher total mass. The single particle levels inside a cavity (as for the MIT bag model) or for ordinary nuclei or hypernuclei show the same order of levels for the lowest eigenstates. First, there is a $1s_{1/2}$ shell, then the $1p_{3/2}$ and the $1p_{1/2}$ shells follow. Due to relativistic effects, the spin-orbit splitting is quite sizable for nucleons. As the quarks are much lighter and relativistic effects are even more pronounced, the spin-orbit splitting for quarks is at the order of 100 MeV for very light bags, i.e. on a similar scale as the splitting between the s and p shell. One can put 6 quarks in the s-shell due to the color degree of freedom, then 12 quarks in the $1p_{3/2}$ shell and again 6 quarks in the $1p_{1/2}$ shell. The smallest and most pronounced magic numbers for quarks are then 6, 18, and 24 (the next one would be already at 42).

Studying isospin asymmetric systems reveals another important effect. The weak nucleon decay by emitting a proton carries away positive charge. Nevertheless, the neutron does not carry away negative charge if it is not accompanied by a π^- . But this decay is suppressed by the mass of the pion and the phase space of the three body final state. Therefore, a strangelet stable against weak nucleon decay is most likely to be negatively charged.

Let us look now for strangelets which have closed shells for all three quark species with a negative charge and a high strangeness fraction as these are the most likely candidates. The first magic strangelet is the quark alpha with 6 quarks of each quark species at $A = 6$ which has zero charge [22]. The magic strangelets with a high strangeness fraction and a negative charge are then at $A = 10, Z = -4$ (with 6 up, 6 down and 18 strange quarks), $A = 12, Z = -6$ (with 6 up, 6 down and 24 strange quarks), $A = 14, Z = -8$ (with 6 up, 18 down and 18 strange quarks), and $A = 16, Z = -10$ (with 6 up, 18 down and 24 strange quarks). One sees a correlation, that adding two units of baryon number decreases the charge by two. These strangelets have a rather high and negative charge fraction of $Z/A \approx -0.5$ very similar to an antideuteron but with a much higher mass and charge! These strangelets constitute a valley of stability which is due to pronounced shell effects.

This picture holds, i.e. these candidates remain, also within an explicit calculation using the MIT bag model with shell mode filling [92]. We calculated the masses of strangelets with all possible combinations of up, down and strange quarks up to a baryon number of $A = 30$. Then we look for possible strong decays as the emission of baryons ($p, n, \Lambda, \Sigma^-, \Sigma^+, \Xi^-, \Xi^0, \Omega^-$) and mesons (pions and kaons) by calculating the mass difference between the strangelet and

its possible decay products. For the strong interactions, we also allow for multiple hadron emission, like the strong decay of a strangelet via a neutron and a pion, and the complete evaporation to hadrons. For example, the strong proton decay $Q' \rightarrow Q + p$ is checked by

$$M(A, S, Z) < M(A - 1, S, Z - 1) + m_p \quad (91)$$

where $M(A, S, Z)$ stands for the mass of the strangelet for a given baryon number, strangeness and charge. Afterwards we check for weak hadronic decay, the single emission of baryons and mesons within the same procedure simply by changing one unit of strangeness in the final products. The weak proton decay $Q' \rightarrow Q + p$ is now checked by

$$M(A, S, Z) < M(A - 1, S \pm 1, Z - 1) + m_p \quad (92)$$

where we allow for both strangeness changing processes of $\Delta S = \pm 1$. This calculation has been done for several bag parameters. We choose a strange quark mass of $m_s = 150$ MeV if not otherwise stated. The value of $B^{1/4} = 145$ MeV and $m_s = 280$ MeV is taken from the original MIT bag model fit to the hadron masses.

The candidates which are stable against strong and weak hadronic decay are plotted in Fig. 26 in a scatter plot as a function of their baryon number and charge fraction. In all the parametrizations shown, we find the candidates at $A = 10$ with $Z = -4$, at $A = 12$ with $Z = -6$, and at $A = 16$ with $Z = -10$. We do not find any candidates for a bag parameter of $B^{1/4} = 180$ MeV or higher as strange quark matter starts to get unstable.

As expected and outlined before, the main long-lived strangelets stable against strong and weak hadronic decay are lying in the valley of stability and are highly negatively charged. This finding is contrary to the common belief that strangelets have a small positive charge and will have serious impact on present heavy ion searches for strange matter. These long-lived candidates are still unstable against weak semileptonic decay (emission of electrons and antineutrinos) and thus will live on a timescale of maybe 10^{-4} sec [93].

One can also ask about the much richer spectrum of short-lived candidates which do decay by weak hadronic processes and thus probably do live only as short as the hyperons ($\tau \approx 10^{-10}$ s). MEMOs can decay weakly on the timescale of the free hyperon weak decay and are thus also belonging to the short-lived candidates. MEMOs have quite distinct properties, they can be negatively charged while carrying a positive baryon number due to the negatively charged hyperons, the Σ^- and the Ξ^- [92]. Light candidates are the combinations $\{2n, 2\Lambda, 2\Xi^-\}$, $\{2p, 2\Lambda, 2\Xi^0\}$, $\{2\Lambda, 2\Xi^0, 2\Xi^-\}$, $_{\Xi^0}^6\text{He}$ and $_{\Lambda\Lambda}^7\text{He}$ discussed in section 3.

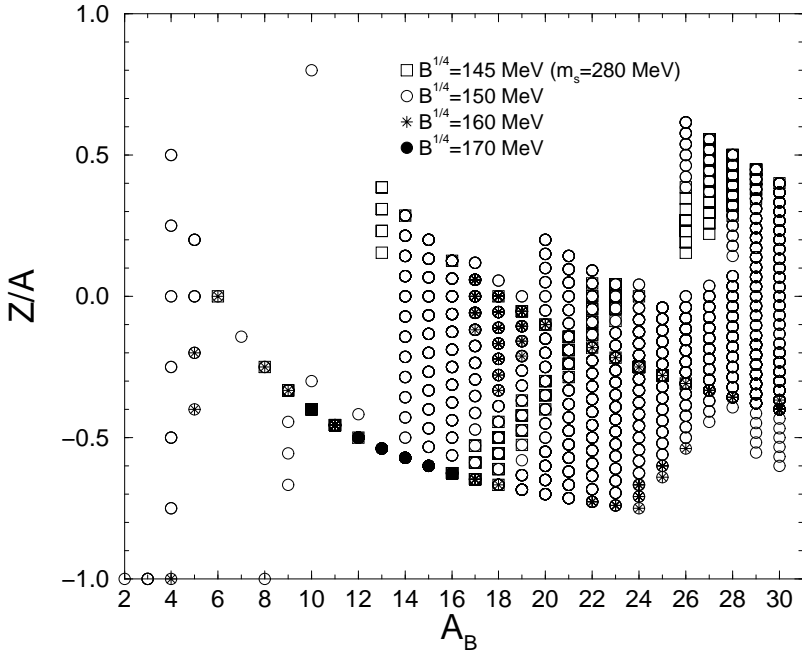


Fig. 26. The charge fraction Z/A for long-lived strangelets, which are stable against strong and weak hadronic decay, for different choices of the bag parameter. The case for the original MIT bag model parameters ($B^{1/4} = 145$ MeV, $m_s = 280$ MeV) is also plotted.

MEMOs thus compete with short-lived strangelets as they are of similar strangeness content. We calculated light MEMOs up to a closed p-shell and checked for metastability (strong decay). We analyzed the strangelet candidates without the weak hadronic decay, i.e. allowing for the strong decay only. The short-lived candidates for MEMOs and strangelets for a bag constant of $B^{1/4} = 160$ MeV are shown in Fig. 27 in a scatter plot as a function of strangeness fraction f_s , charge fraction Z/A and baryon number A .

As can be seen, there are many more short-lived candidates than long-lived. Light MEMOs can have very unusual charge fractions between $Z/A = \pm 0.6$ indicating a rich structure of strange hadronic matter. Strangelet candidates also cover a wide range of charge fraction but are mainly located at negative charge. This comes from the strong decay which shifts strangelets to higher strangeness fraction and to negative charge. There are MEMOs and strangelets with the same strangeness content and baryon number. Here, the energetically least favourable object can decay into the other via strong interactions. A strangelet created in a quark gluon plasma can then possibly decay into a MEMO. Or vice versa, MEMOs can coalesce from the hot and hyperon-rich zone of a relativistic heavy ion collision first and then they form a strangelet.

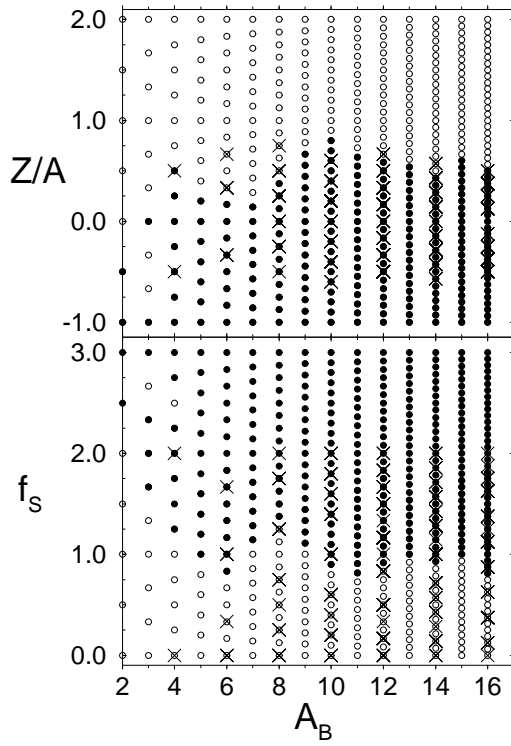


Fig. 27. The strangeness per baryon f_s (lower part) and the charge fraction Z/A (upper part) as a function of the baryon number A_B for short-lived strangelets (dots) and unstable strangelets (open circles) for a bag constant of $B^{1/4} = 160$ MeV. The hadronic counterparts, MEMOs, are shown by crosses.

Presently, there are only experiments designed to look for long-lived composites with a lifetime of $\tau > 50$ ns. Designing an experiment for short-lived composites is challenging but planned for future colliders and can reveal the possibly rich structure of strange matter.

5 STRANGE MATTER IN NEUTRON STARS

Originally (strange) quark matter in bulk was thought to exist only in the interior of neutron stars where the pressure is high enough so that the neutron matter melts into its quark substructure [18,19,15]. At least in the cores of neutron stars (where the density rises up to the order of 10 times normal nuclear density) it is not very likely that matter consists of individual hadrons. For an overview of the structure of neutron stars see [2,94,95].

On the other hand it is also known that the pure ‘neutron’ matter is not really a nuclear matter state made solely out of neutrons, but at least at higher densities consists also of a considerable amount of protons as well as hyperons. The extrapolation of strange hadronic matter to higher densities in fact has influence on the constituents of ‘neutron’ matter. The gross structure of a neutron star like its mass M and radius R is influenced by the composition of its stellar material. This holds especially in the case of the existence of strangeness bearing “exotic” components like hyperons or strange quark matter which may significantly change the characteristic mass-radius (MR) relation of the star.

In this final section we therefore address briefly on how the two different forms of strange matter might influence the properties of neutron stars. This section, however, can only give an impression of its implication on neutron star physics. It is based primarily on some own work on this interesting issue and can thus provide only an idea of possible effects. The interested reader should therefore also consult the cited literature for a much wider range of topics.

5.1 *Strange quark matter stars*

In section 2 we have described the equation of state of cold strange quark matter by means of a simple noninteracting Fermi gas of up, down and strange quarks. In the following we adopt a somewhat modified model which was developed quite recently, the effective mass bag model [96]:

In condensed matter as well as in nuclear physics medium effects play an important role. One of the most prominent medium effects are effective masses generated by the (average) interaction of the particles with the system. For example in the case of a gluon gas at high temperature the consideration of an effective mass for the gluon within the ideal gas approximation leads to an excellent description of the equation of state found in lattice calculations [97,98]. If one considers now analogously the case of a quark gas at zero temperature the situation is as follows: The quarks are considered now as dressed quasi-particles which acquire an effective mass by the interaction with the other quarks of the dense system. The effective quark masses are obtained

from the zero momentum limit of the quark dispersion relation, which follows from the so called hard dense loop (HDL) approximation of the one-loop quark self-energy at finite chemical potential [99,96]. They are given by

$$m_q^{*2}(\mu) = \frac{g^2 \mu^2}{6\pi^2} \quad (93)$$

for the light quarks (i.e. u,d -quarks) and

$$m_s^*(\mu) = \frac{m_s}{2} + \sqrt{\frac{m_s^2}{4} + \frac{g^2 \mu^2}{6\pi^2}} \quad (94)$$

for massive quarks with current quark mass m_s (s -quarks). g denotes the QCD coupling constant and is treated as a further phenomenological parameter as in the MIT model. As can be readily expected from the formulas (93) and (94), the effective masses increase with the coupling constant g and the quark chemical potential μ . These effective masses are used in the ideal Fermi gas EOS at temperature $T = 0$. Similar to the expressions stated in section 2, the pressure, the particle density ρ and energy density ϵ of this quasiparticle Fermi gas take the following form

$$\begin{aligned} p(\mu) + B^*(\mu) &= \frac{d}{2\pi^2} \int_{k=0}^{k_F} dk k^2 (\mu - \omega^*(k)) \\ &= \frac{d}{24\pi^2} \left[\mu k_F \left(\mu^2 - \frac{5}{2} m^{*2} \right) + \frac{3}{2} m^{*4} \ln \left(\frac{k_F + \mu}{m^*} \right) \right] , \end{aligned} \quad (95)$$

$$\rho(\mu) = \frac{d}{6\pi^2} k_F^3 , \quad (96)$$

$$\epsilon(\mu) - B^*(\mu) = \frac{d}{16\pi^2} \left[\mu k_F \left(2\mu^2 - m^{*2} \right) - m^{*4} \ln \left(\frac{k_F + \mu}{m^*} \right) \right] . \quad (97)$$

Here d denotes the degree of degeneracy (e.g. $d = 6n_f$ for n_f flavors). Up to the additional function B^* , which can be regarded as a μ -dependent bag constant, these are the ideal Fermi gas formulas at temperature $T = 0$ for quasiparticles of mass m^* and chemical potential μ . Due to the μ -dependence of $m^*(\mu)$ the introduction of the function $B^*(\mu)$ is necessary in order to maintain thermodynamic self-consistency on the one hand and to receive the final expressions (as given above) for the particle and energy density on the other hand, having the exact form as a noninteracting, but massive Fermi gas [96]. The MIT bag constant B_0 still enters as $B^*(\mu = 0)$ and is thus a further phenomenological parameter of the model. When inspecting this improved equation of state

for strange matter numerically, the overall energy per baryon number E/A increases for increasing coupling constant g [96]. This behavior one would intuitively expect as the masses of the quarks do increase with the coupling constant. In return, strange matter thus becomes less energetically favorable for realistic QCD coupling constants $\alpha_s = \frac{g^2}{4\pi}$. (One should be aware, however, that the value of the ‘free’ bag parameter is still far from being settled. For example, the results of Peshier et al. [98] suggest, that, by including effective medium masses in describing the hot gluon plasma and compare it to lattice calculations, the employed free bag parameter $B_0^{1/4} \approx 0.7T_c$ might still be considerably smaller than even the already very low original MIT bag constant of $B_0^{1/4} = 145$ MeV. In this sense, all the speculative conclusions of section 2 are all still valid.)

We now show how a neutron star would look like under the assumption that it *entirely* consists of cold electrically charge neutral SQM in equilibrium with respect to the weak interactions.

This requires the inclusion of electrons into the model. The thermodynamics of electrons at $T = 0$ can be described by a relativistic Fermi gas

$$\rho_e = \frac{\mu_e^3}{3\pi^2} \quad (98)$$

$$\epsilon_e = \frac{\mu_e^4}{4\pi^2} \quad (99)$$

$$p_e = \frac{\mu_e^4}{12\pi^2}. \quad (100)$$

In return, one has four chemical potentials ($\mu_u, \mu_d, \mu_s, \mu_e$) which are related by the chemical equilibrium between the quark flavors and the leptons. The basic weak reactions are given by



The equilibration of flavors is provided by



Hence, the four chemical potentials are reduced to two independent ones

$$\mu \equiv \mu_s = \mu_d \quad \text{and} \quad \mu_u = \mu - \mu_e. \quad (104)$$

Finally, the overall condition of electrically charge neutrality (‘neutron’ stars

are locally charge neutral)

$$2/3\rho_u - 1/3(\rho_d + \rho_s) - \rho_e = 0 \quad (105)$$

just leaves one independent chemical potential, say μ . Therefore, the EOS can be written as a function of μ only:

$$\rho_B = (\rho_u + \rho_d + \rho_s)/3, \quad (106)$$

$$\epsilon = \epsilon_u + \epsilon_d + \epsilon_s + \epsilon_e + B_0, \quad (107)$$

$$p = p_u + p_d + p_s + p_e - B_0. \quad (108)$$

In the following we assume a cold, static, spherical star. It is described by the solutions of the famous Oppenheimer-Volkoff-Tolman (OVT) equations of hydrostatic equilibrium:

$$\frac{dp(r)}{dr} = -\frac{\epsilon(r)m(r)}{r^2} \left(1 + \frac{p(r)}{\epsilon(r)}\right) \left(1 + \frac{4\pi p(r)r^3}{m(r)}\right) \left(1 - \frac{2m(r)}{r}\right)^{-1},$$

$$\frac{dm(r)}{dr} = 4\pi r^2 \epsilon(r). \quad (109)$$

They follow from general relativity [100] which one has to apply due to highly concentrated matter and therefore curved space-time. The solutions of the OVT equations are the pressure $p(r)$ and mass $m(r)$ inside a sphere of radius r . The total radius R of the star is determined by the condition $p(R) = 0$ while the total gravitating mass of the star is given by

$$M = \int_{r=0}^R 4\pi r^2 \epsilon(r) dr. \quad (110)$$

The OVT equation can be solved specifying the central energy density $\epsilon_c = \epsilon(r=0)$ and the EOS in the form $p = p(\epsilon)$.

In Fig. 28 the MR relation of such a hypothetical star is depicted. The numerical calculation of $p = p(\epsilon)$ from (107) and (108) shows that there is no noteworthy influence by a change of the coupling constant g . The EOS gets slightly softer for high values of the coupling constant (e.g. $g = 4$) but there is no remarkable impact on R and M (see Fig. 28). The maximum mass of such a star lies in the range of 1.6-2 times the solar mass and is thus compatible with the predictions of normal (nonexotic) neutron stars. One should also note one special feature inherent to the description of pure quark matter stars. As they are inherent self-bound as a possible consequence of QCD (which just corresponds to the speculation about the existence of stable quark matter),

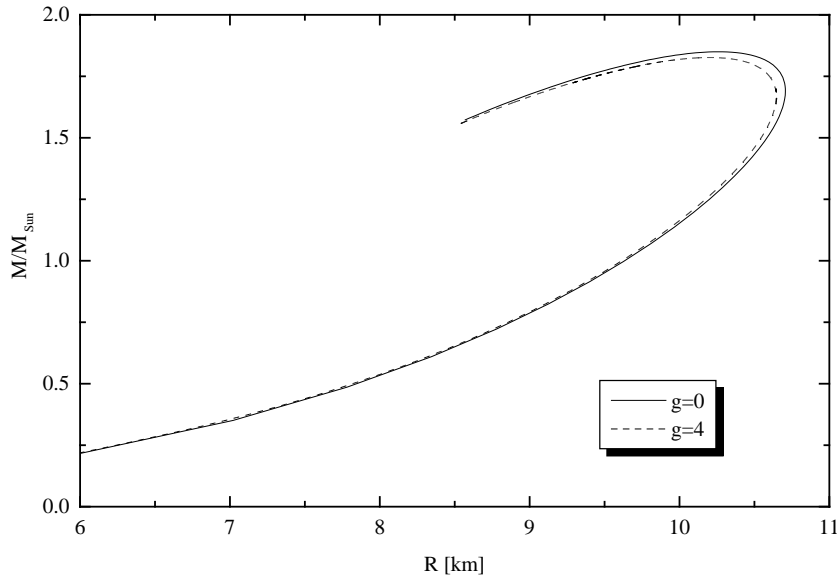


Fig. 28. Mass M/M_{\odot} (in units of solar mass) versus radius R of a SQM star, $m_s = 150\text{MeV}$, $B_0^{1/4} = 145\text{MeV}$.

for smaller masses $M \lessapprox M_{\text{sun}}$, the quark matter stars do become also smaller. This is different, however, for normal neutron stars, where their size typically increases for lower masses due to the very diffuse (i.e. low density) surface.

Furthermore, Fig. 29 shows the change of the strangeness fraction versus the baryon density for different values of g . Throughout the interior the quark matter is indeed strange, with a net strangeness content of $f_s \approx 0.7 - 0.9$. Therefore the quark matter star is in fact a strange quark matter star.

Note, however, that the illustrative results are only valid under the assumption of a pure SQM star. Although there is no change in mass and radius of the star, there is, nevertheless, an increase of the energy E/A at a given radius inside the star due to medium effects. Owing to the increase of E/A in the entire star a phase transition to hadronic matter will take place at a smaller radius in the interior of the star [94,101]. The ‘neutron’ star would then have the form of a so called hybrid star, i.e. a star which is made of baryonic matter in the outer region, but with a quark matter core in the deep interior. It would be interesting to see how the presented improved equation of state will affect the picture of such a hybrid star. Such a study has recently been carried out [102]. The deconfinement phase transition from hadronic matter to the SQM phase is constructed according to a construction proposed by Glendenning [103,95]. One here requires the weaker condition of global charge neutrality instead of assuming charge neutrality in either phase. The latter assumption would

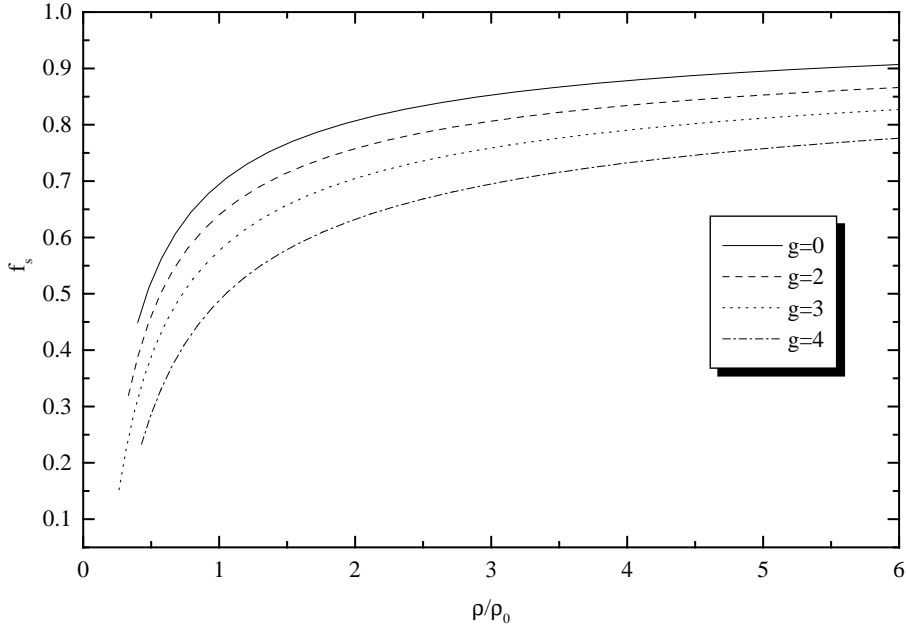


Fig. 29. Strangeness fraction f_s versus ρ/ρ_0 in a SQM star, $m_s = 150\text{MeV}$, $B_0^{1/4} = 145\text{MeV}$ and $\rho_0 = 0.17\text{fm}^{-3}$.

have the drastic consequence of strictly excluding a spatial extended region of possible mixed phase inside the star due to a resulting *constant* pressure in the mixed phase. In the mixed phase, however, the fraction of the quark matter phase on the one side, and the fraction of the hadronic matter phase on the other side, might both be (oppositely) charged if only their volume proportion χ is always chosen to fulfill the condition of global charge neutrality

$$\chi q_{QP} + (1 - \chi) q_{HP} = 0. \quad (111)$$

Here q_{QP} and q_{HP} denotes the charge density of each phase. (This argument of Glendenning is very similar in its spirit to that one given in section 3 concerning the idea of strangeness separation during the mixed phase in the QGP phase transition.) Since the pressure inside a star must fall monotonically from its interior to its surface, a constant pressure mixed phase could not exist over a finite region inside the star. However, with the above description (which is the thermodynamic correct one) one finds that the pressure varies smoothly and continuously with the proportion of phases in equilibrium [103,95] leading to a mixed phase of finite radial extent inside the star.

In Fig. 30 the schematic view of possible hybrid stars of (an assumed and fixed) canonical mass of $M = 1.4 M_\odot$ is shown for different and increasing coupling constant g . The bag constant was chosen so that a pure quark matter

Fig. 30. Radii and inner structure of a hybrid star of mass $M = 1.4M_\odot$ ($m_s = 150\text{MeV}$, $B_0^{1/4} = 165\text{MeV}$) [104].

star cannot exist even for $g = 0$. The hadronic phase is described within the Walecka model including (some) hyperon degrees of freedom. (Details will not be given here and we refer to [102].) One finds that already a small coupling constant of $g = 1.5$ ($\alpha_s \approx 0.18$) is able to halve the radius of the pure SQM core (denoted as QP) of initially $R \approx 6\text{ km}$ (with neglected medium effects, Fig. 30a) to $R \approx 3\text{ km}$ (Fig. 30c). Already at $g = 2$ ($\alpha_s \approx 0.32$) the pure SQM core has completely vanished (Fig. 30d), while the pure hadron phase (HP) has grown only moderately. SQM is now only present in the mixed phase (MP) which dominates the interior structure of the star. For $g \approx 3.5$ a phase transition to SQM and thus the occurrence of the mixed phase is completely suppressed.

5.2 Strange hadronic matter inside neutron stars

As shown in the previous section, strange quark matter can appear in the core of a neutron star. Here we will discuss the scenario that strange hadrons, as hyperons and kaons, can appear in the interior of a neutron star. Indeed, it was shown by Glendenning that hyperons [105] appear at a moderate density of about $2 \div 3$ times normal nuclear matter density $\rho_0 = 0.15\text{ fm}^{-3}$. These new species influence the properties of the equation of state of matter and the global properties of neutron stars. There are so many hyperons in the neutron star that the whole object is more appropriately dubbed a giant hypernucleus.

Hyperons considerably soften the EOS and reduce the maximum mass of a neutron star.

The appearance of another form of hadrons with strangeness, kaon condensates, was discussed also in many papers [106–110]. Chiral perturbation theory (ChPT) gives a rather robust prediction of the onset of antikaon condensation at $\rho \approx (3 - 4)\rho_0$ [107] taking into account in-medium modifications of the antikaon energy with density. Antikaon condensation will soften the EOS and reduce the maximum mass of a neutron star similar to the case of hyperons. This will allow for the existence of low-mass black holes and implications have been discussed in [111]. In [112,113] it was criticized that effects nonlinear in density were not taken into account which will shift the appearance of a kaon condensed phase to higher density. Moreover, hyperons were not considered in this approach.

Rather recently, antikaons and hyperons were considered on the same footing, where it was found that hyperons shift the onset of antikaon condensation to higher density [108] or that it is very unlikely that it appears at all due to the rather strong hyperon-hyperon interactions [109].

In the following we will discuss the appearance of hyperons and kaons in neutron star matter.

The equation of state for neutron star matter is derived by standard methods (see e.g. ref. [105] for the RMF approach without the hidden strange meson fields). The equations of motion for the meson fields in uniform matter at rest are given by

$$\begin{aligned}
m_\sigma^2 \sigma + \frac{\partial}{\partial \sigma} U(\sigma) &= \sum_B g_{\sigma B} \rho_S^{(B)} \\
m_{\sigma^*}^2 \sigma^* &= \sum_B g_{\sigma^* B} \rho_S^{(B)} \\
m_\omega^2 V_0 + dV_0^3 &= \sum_B g_{\omega B} \rho_V^{(B)} \\
m_\rho^2 R_{0,0} &= \sum_B g_{\rho B} \tau_0^B \rho_V^{(B)} \\
m_\phi^2 \phi_0 &= \sum_B g_{\phi B} \rho_V^{(B)} \quad .
\end{aligned} \tag{112}$$

where ρ_S and ρ_V denote the scalar and vector densities, respectively. The equations can be solved for a given total baryon density ρ_B and charge density ρ_c including the contributions from the free electrons and muons

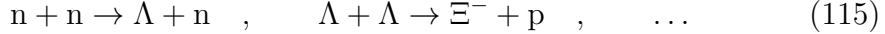
$$\rho_B = \sum_B \rho_V^{(B)}$$

$$\rho_c = \sum_B q_B \rho_V^{(B)} + \sum_{l=e,\mu} q_l \rho_l = 0 \quad (113)$$

where q_i stands for the electric charge of a species i . In β -equilibrium the chemical potentials of the particles are related to each other by

$$\mu_i = b_i \cdot \mu_B + q_i \cdot \mu_e \quad (114)$$

where b_i is the baryon number of a species i . This means that all reactions which conserve charge and baryon number are allowed, as e.g.



Since we consider neutron stars on a long time scale, the strangeness quantum number is not constrained and the net strangeness is determined by the condition of β -equilibrium. The above equations fix the fields and the equilibrium composition of neutron star matter.

Fig. 31 shows the composition of neutron star matter for the parameter set TM1 with hyperons including the hyperon-hyperon interactions. Up to the maximum density considered here all effective masses remain positive and no instability occurs. The proton fraction has a plateau at $(2 - 4)\rho_0$ and exceeds 11% which allows for the direct URCA process and a rapid cooling of a neutron star. Hyperons, first Λ 's and Σ^- 's, appear at $2\rho_0$, then Ξ^- 's are populated already at $3\rho_0$. The number of electrons and muons has a maximum here and decreases at higher densities, i.e. the electrochemical potential decreases at high densities. The fractions of all baryons show a tendency towards saturation, they asymptotically reach similar values corresponding to spin-isospin and hypercharge-saturated matter. Hence, a neutron star is more likely a giant hypernucleus [105]!

In the following we adopt the meson-exchange picture for the KN-interaction simply because we use it also for parametrizing the baryon interactions. We start from the following Lagrangian

$$\mathbf{L}_{KN}^{\text{RMF}} = D_\mu^* \bar{K} D^\mu K - m_K^2 \bar{K} K - g_{\sigma K} m_K \bar{K} K \sigma - g_{\sigma^* K} m_K \bar{K} K \sigma^* \quad (116)$$

with the covariant derivative

$$D_\mu = \partial_\mu + ig_{\omega K} V_\mu + ig_{\rho K} \vec{\tau} \vec{R}_\mu + ig_{\phi K} \phi_\mu \quad . \quad (117)$$

The scalar fields essentially decrease the kaon mass, while the vector fields will increase (decrease) the energy of the kaon (antikaon) in the dense medium. The scalar coupling constants are fixed by the s-wave KN-scattering lengths.

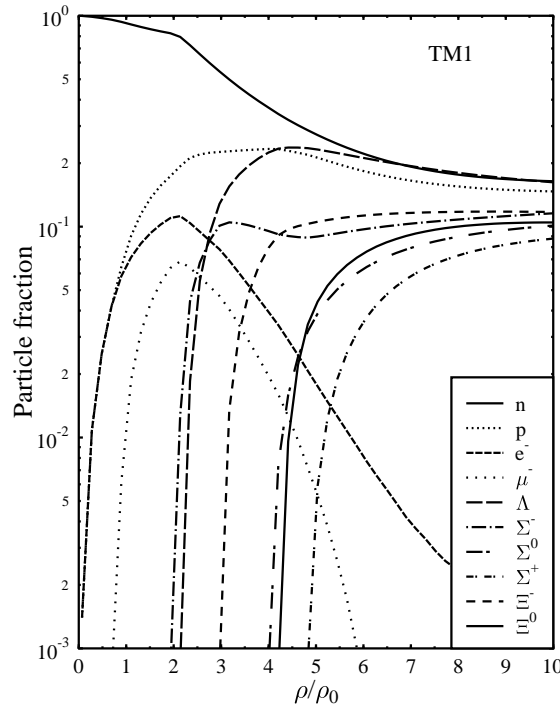


Fig. 31. The composition of neutron star matter with hyperons which appear abundantly in the dense interior (from Ref. [109]).

The coupling constants to the vector mesons are chosen from SU(3)-relations. The onset of s-wave kaon condensation is now determined by the condition $-\mu_e = \mu_{K^-} \equiv \omega_{K^-}(k=0)$.

The density dependence of the K and \bar{K} effective energies is displayed in Fig. 32. The energy of the kaon is first increasing in accordance with the low density theorem. The energy of the antikaon is decreasing steadily at low densities. With the appearance of hyperons the situation changes dramatically. The potential induced by the ϕ -field cancels the contribution coming from the ω -meson. Hence, at a certain density the energies of the kaons and antikaons become equal to the kaon (antikaon) effective mass, i.e. the curves for kaons and antikaons are crossing at a sufficiently high density. At higher densities the energy of the kaon gets even lower than that of the antikaon! Since the electrochemical potential never reaches values above 160 MeV here antikaon condensation does not occur at all. The possibility of antikaon condensation was checked for several parameter sets and found that at least 100 MeV are missing for the onset of kaon condensation [109]. This is in contrast to previous calculations disregarding hyperons [107] but in line with the findings in [108] where it was seen that hyperons shift the critical density for kaon condensation to higher density.

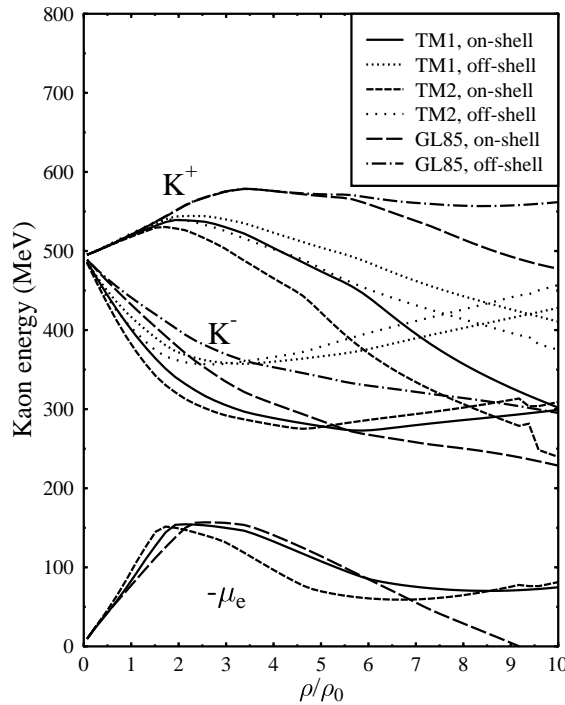


Fig. 32. The effective energy of the kaon and the antikaon and the electrochemical potential. Kaon condensation does not occur over the whole density region considered (from Ref. [109]).

These illustrations clearly demonstrate the ‘richness’ of possible scenarios for the interior structure of neutron stars. In return it represents a very interesting and still open and lively field to pin down the possible structure of neutron stars by its observed properties and phenomena.

Acknowledgments:

J. S.-B. thanks the Alexander von Humboldt Stiftung for its support with a Feodor Lynen scholarship. Thanks go to our friends and colleagues A. Diener, C. Dover, A. Gal, P. Koch-Steinheimer, I. Mishustin, D. Rischke, K. Schertler, M. Thoma and especially to H. Stöcker. Without their help and collaboration this work would not have been possible. This work is supported in part by the Director, Office of Energy Research, Office of High Energy and Nuclear Physics, Nuclear Physics Division of the U.S. Department of Energy under Contract No. DE-AC03-76SF00098.

References

- [1] for a general introduction into the field see:
Henry J. Crawford and Carsten H. Greiner, ‘The Search for Strange Matter’, *Scientific American* **270** (1), (1994) 58.
- [2] for a detailed survey on the (astro-)physical implications see:
‘Strange Quark Matter in Physics and Astrophysics’, edited by J. Madsen and P. Haensel, *Nucl. Phys. B (Proc. Suppl.)* **24B**; ‘Strangeness and Quark Matter’, Proceedings of the International Symposium, Krete, Greece, 1994, edited by G. Vassiliadis, A. Panagiotou, B. Shiva Kumar and J. Madsen, World Scientific, 1995; Proceedings of the International Symposium on Strangeness in Quark Matter, Santorini, Greece, 1997, *J. Phys.* **G23**
- [3] C. Greiner, P. Koch and H. Stöcker, *Phys. Rev. Lett.* **58**, 1825 (1987).
- [4] C. Greiner, D.-H. Rischke, H. Stöcker and P. Koch, *Z. Phys. C* **38**, 283 (1988); *Phys. Rev. D* **38**, 2797 (1988).
- [5] C. Greiner and H. Stöcker, *Phys. Rev. D* **44**, 3517 (1991).
- [6] P. Koch, B. Müller, and J. Rafelski, *Phys. Rep.* **142**, 167 (1986).
- [7] T. Matsui and H. Satz, *Phys. Lett.* **178B**, 416 (1986).
- [8] A. R. Bodmer, *Phys. Rev. D* **4**, 1601 (1971).
- [9] S. A. Chin and A. K. Kerman, *Phys. Rev. Lett.* **43**, 1292 (1979).
- [10] J. D. Bjorken and L. D. McLerran, *Phys. Rev. D* **20**, 2353 (1979).
- [11] E. Witten, *Phys. Rev. D* **30**, 272 (1984).
- [12] A. De Rujula and S.L. Glashow, *Nature* **312**, 734 (1984); A. De Rujula, *Nucl. Phys. A* **434**, 605c (1985).
- [13] E. Farhi and R. L. Jaffe, *Phys. Rev. D* **30**, 2379 (1984).
- [14] We thank F. Weber and N. Glendenning for providing us with Fig. 3.
- [15] B. A. Freedman and L. D. McLerran, *Phys. Rev. D* **16**, 1169 (1978).
- [16] T. DeGrand, R. L. Jaffe, K. Johnson and J. Kiskis, *Phys. Rev. D* **12**, 2060 (1975).
- [17] In later papers, like e.g. in reference [13], the fine structure constant has been redefined to $\alpha_c = g_c^2/4\pi$, so that the original MIT parameter would there have to be taken as $\alpha_c = 2.2$.
- [18] J. C. Collins and M. J. Perry, *Phys. Rev. Lett.* **34**, 1353 (1975).
- [19] G. Baym and S. Chin, *Phys. Lett.* **62B**, 241 (1976).

[20] C. Alcock and E. Farhi, Phys. Rev. **D32**, 1273 (1985); G. Baym, E.W. Kolb, L. McLerran, T.P. Walker and R.L. Jaffe, Phys. Lett. **B160**, 181 (1985); F. Halzen and H.C. Liu, Phys. Rev. **D32**, 1716 (1985); P.B. Price, Phys. Rev. **D38**, 3813 (1988); O.G. Bevenuto and J.E. Horvath, Phys. Rev. Lett. **63**, 716 (1989); T. Saito, Y. Hatano, Y. Fukada and H. Ota, Phys. Rev. Lett. **65**, 2094 (1990).

[21] D. Vasak, L. Neise and W. Greiner, Phys. Rev. **C34**, 1308 (1986).

[22] F. C. Michel, Phys. Rev. Lett. **60**, 677 (1988).

[23] R. L. Jaffe, Phys. Rev. Lett. **38**, 195 (1977), 617(E); see also the contribution of Jaffe in the proceedings [2].

[24] R.E. Chrien and C.B. Dover, Ann. Rev. Nucl. Part. Sci. **39**, 113 (1989).

[25] H. Bandō, T. Motoba and J. Žofka, Int. J. Mod. Phys. **A5**, 4021 (1990).

[26] M. Danysz and J. Pniewski, Phil. Mag. **44**, 348 (1953).

[27] G.C. Bonnazzola, T. Bressani, R. Cester, E. Chiavassa, G. Dellacasa, A. Fainberg, N. Mirfakhrai, A. Musso and G. Rinaudo, Phys. Lett. **B53**, 297 (1974).

[28] W. Brückner et al., Phys. Lett. **62B**, 481 (1976).

[29] T. Motoba, H. Bandō, R. Wünsch and J. Žofka, Phys. Rev. **C38**, 1322 (1988).

[30] C. Milner et al., Phys. Rev. Lett. **54**, 1237 (1985).

[31] P.H. Pile et al., Phys. Rev. Lett. **66**, 2585 (1991).

[32] M. Akei et al., Il Nuovo Cim. **102A**, 457 (1989).

[33] H. Feshbach, Nucl. Phys. **A507**, 219c (1990).

[34] R. Bertini et al., Phys. Lett. **83B**, 306 (1979).

[35] D.J. Millener, A. Gal, C.B. Dover and R.H. Dalitz, Phys. Rev. **C31**, 499 (1985).

[36] D.J. Millener, C.B. Dover and A. Gal, Phys. Rev. **C38**, 2700 (1988).

[37] A. Bouyssy, Nucl. Phys. **A290**, 159 (1977)
A. Bouyssy, Nucl. Phys. **A381**, 445 (1982).

[38] R. Brockmann and W. Weise, Phys. Lett. **69B**, 167 (1977)
R. Brockmann and W. Weise, Nucl. Phys. **A355**, 364 (1981).

[39] J. Boguta and S. Bohrmann, Phys. Lett. **102B**, 93 (1981).

[40] M. Rufa, H. Stöcker, P.-G. Reinhard, J. Maruhn and W. Greiner, J. Phys. **G13**, L143 (1987).

[41] J. Mareš and J. Žofka, Z. Phys. **A333**, 209 (1989).

[42] M. Rufa, J. Schaffner, J. Maruhn, H. Stöcker, W. Greiner and P.-G. Reinhard, Phys. Rev. **C42**, 2469 (1990).

- [43] P.D. Barnes, Nucl. Phys. **A479**, 89c (1988).
- [44] S. Polikanov, Nucl. Phys. **A478**, 805c (1988).
- [45] C.J. Batty, E. Friedman and A. Gal, Phys. Lett. **B335**, 273 (1994).
- [46] R.S. Hayano, Nucl. Phys. **A508**, 99c (1990).
- [47] C.B. Dover and A. Gal, Ann. Phys. **146**, 309 (1983).
- [48] J. Schaffner, C.B. Dover, A. Gal, D.J. Millener, C. Greiner and H. Stöcker, Ann. of Phys. (N.Y.) **235**, 35 (1994).
- [49] R.H. Dalitz, D.H. Davies, P.H. Fowler, A. Montwill, J. Pniewski and J.A. Zakrzewski, Proc. Roy. Soc. Lond. **A426**, 1 (1989).
- [50] D.J. Prowse, Phys. Rev. Lett. **17**, 782 (1966).
- [51] M. Danysz et al., Phys. Rev. Lett. **11**, 29 (1963)
M. Danysz et al., Nucl. Phys. **49**, 121 (1963).
- [52] S. Aoki et al., Prog. Theor. Phys. **85**, 1287 (1991).
- [53] C.B. Dover, D.J. Millener, A. Gal and D.H. Davis, Phys. Rev. **C44**, 1905 (1991).
- [54] B.D. Serot and J.D. Walecka, Adv. Nucl. Phys. **16**, 1 (1986).
- [55] P.-G. Reinhard, Rep. Prog. Phys. **52**, 439 (1989).
- [56] B.D. Serot, Rep. Prog. Phys. **55**, 1855 (1992).
- [57] J. Boguta and A.R. Bodmer, Nucl. Phys. **A292**, 413 (1977).
- [58] P.-G. Reinhard, Z. Phys. **A329**, 257 (1988).
- [59] J. Blocki and M. Flocard, Nucl. Phys. **A273**, 45 (1976).
- [60] M. Rufa, P.-G. Reinhard, J. Maruhn, W. Greiner and M.R. Strayer, Phys. Rev. **C38**, 390 (1988).
- [61] P.-G. Reinhard, M. Rufa, J. Maruhn, W. Greiner and J. Friedrich, Z. Phys. **A323**, 13 (1986).
- [62] J. Schaffner, C. Greiner and H. Stöcker, Phys. Rev. **C46**, 322 (1992).
- [63] J. Schaffner, C.B. Dover, A. Gal, C. Greiner and H. Stöcker, Phys. Rev. Lett. **71**, 1328 (1993).
- [64] C.B. Dover and A. Gal, Prog. Part. Nucl. Phys. **12**, 171 (1984).
- [65] A.v. Keitz, H. Sorge, R. Mattiello, H. Stöcker and W. Greiner, Phys. Lett. **B243**, 7 (1990).
- [66] J. Rafelski and B. Müller, Phys. Rev. Lett. **48**, 1066 (1982); **56**, 2334(E) (1986).
- [67] J. Kapusta and A. Mekjian, Phys. Rev. **D33**, 1304 (1986); T. Matsui, B. Svetitsky and L. D. McLerran, Phys. Rev. **D34**, 783, 2047 (1986).

[68] T. Abbott et al. (E802 Collab.), *Phys. Rev. Lett.* **64**, 847 (1990); *Phys. Rev. Lett.* **66**, 1567 (1991); O. Hansen, *Comm. Nucl. Part. Phys.* **20**, 1 (1992).

[69] S. Abatzis et al. (WA85 Collab.), *Phys. Lett.* **B316**, 615 (1993); *Nucl. Phys.* **A566**, 225c (1994); J. B. Kinson et al. (WA85 Collab.), *Nucl. Phys.* **A544**, 321c (1992).

[70] E. Andersen et al. (NA36 Collab.), *Phys. Lett.* **B294**, 127 (1992); *Phys. Rev.* **C46**, 727 (1992), *Phys. Lett.* **B327**, 433 (1994).

[71] M. Gazdzicki et al. (NA35 Collab.), *Nucl. Phys.* **A566**, 503c (1994); T. Alber et al. (NA35 Collab.), *Z. Phys. C* **64**, 195 (1994).

[72] R. Mattiello, H. Sorge, H. Stöcker and W. Greiner, *Phys. Rev. Lett.* **63**, 1459 (1989).

[73] H. Sorge, M. Berenguer, H. Stöcker and W. Greiner, *Phys. Lett.* **B289**, 6 (1992).

[74] K. Werner and J. Aichelin, *Phys. Lett.* **B308**, 372 (1993); *Phys. Lett.* **B300**, 158 (1993).

[75] C. Greiner and B. Müller, *Phys. Lett.* **B219**, 199 (1989).

[76] M. Gyulassy, *Phys. Lett.* **B286**, 211 (1992).

[77] H. Liu and G. L. Shaw, *Phys. Rev.* **D30**, 1137 (1984).

[78] M. Danos and J. Rafelski, *Phys. Rev.* **D27**, 671 (1983).

[79] B. Banerjee, N. K. Glendenning and T. Matsui, *Phys. Lett.* **B127**, 453 (1983).

[80] B. Müller and J. M. Eisenberg, *Nucl. Phys.* **A435**, 791 (1985).

[81] H. W. Barz, J. P. Bondorf, C. Guet, J. Lopez and H. Schulz, *Europhys. Lett.* **4**, 997 (1987).

[82] P. R. Subramanian, H. Stöcker and W. Greiner, *Phys. Lett.* **B137**, 468 (1986). U. Heinz, P. R. Subramanian, H. Stöcker and W. Greiner, *J. Phys. G* **12**, 1237 (1986).

[83] H. W. Barz, B. L. Friman, J. Knoll and H. Schulz, *Nucl. Phys.* **A484**, 661 (1988)

[84] L. van Hove, *Z. Phys. C* **27**, 135 (1985); *Ann. Phys.* **192**, 66 (1989).

[85] G. Bertsch, M. Gong, L. D. McLerran, V. Ruuskanen and E. Sarkkinen, *Phys. Rev.* **D37**, 1202 (1988).

[86] K. S. Lee and U. Heinz, *Phys. Rev.* **D47**, 2068 (1993); in this work the phase transition of strange quark matter was analyzed for all possible strangeness contents at zero and finite temperature within the same model equation of state as originally employed in reference [3,4].

[87] C. Spieles, L. Gerland, H. Stöcker, C. Greiner, C. Kuhn and J.P. Coffin, *Phys. Rev. Lett.* **76**, 1776 (1996).

[88] R. Mattiello, C. Hartnack, A.v. Keitz, J. Schaffner, H. Sorge, H. Stöcker, C. Greiner, Nucl. Phys. B (Proc. Suppl.) **24B**, 221 (1991); M. Sano, M. Wakai, Czech. J. Phys. **42**, 1239 (1992); A.J. Baltz, C.B. Dover, S.H. Kahana, Y. Pang, T.J. Schlagel, E. Schnedermann, Phys. Lett. **B325**, 7 (1994)

[89] J. Sandweiss, Nucl. Phys. B (Proc. Suppl.) **24B**, 234 (1991); F. Rotondo et al., Nucl. Phys. B (Proc. Suppl.) **24B**, 265 (1991); J. Barette et al. (E-814 Collab.), Phys. Lett. **B252**, 550 (1990); B. Shiva Kumar, Nucl. Phys. **A590**, 29c (1995); F. Rotondo et al., Nucl. Phys. **A610**, 297c (1996); T.A. Armstrong et al., Phys. Rev. Lett. **79**, 3612 (1997); T.A. Armstrong et al., Nucl. Phys. **A625**, 494 (1997).

[90] M. Aoki et al., Phys. Rev. Lett. **69**, 2345 (1992); H.J. Crawford et al., Nucl. Phys. B (Proc. Suppl.) **24B**, 251 (1991); D. Beavies et al., Phys. Rev. Lett. **75**, 3078 (1995).

[91] K. Pretzl et al. (NA52 Collab.), Phys. Rev. Lett. **72**, 1415 (1994); W. Volken et al (NA52 Collab.), Nucl. Phys. **A566**, 507c (1994); F. Dittus, Nucl. Phys. **A590**, 347c (1995); G. Applequist et al.; Phys. Rev. Lett. **76**, 3907 (1996); R. Klingenberg et al., Nucl. Phys. **A610**, 306c (1996).

[92] J. Schaffner-Bielich, C. Greiner, A. Diener and H. Stöcker, Phys. Rev. **C55**, 3038 (1997).

[93] H. Heiselberg, J. Madsen and K. Riisager, Phys. Scr. **34**, 556 (1986); P. Koch, Nucl. Phys. B (Proc. Suppl.) **24B**, 255 (1991).

[94] S.L. Shapiro and S.A. Teukolsky, *Black Holes, White Dwarfs, and Neutron Stars*, John Wiley & sons, N.Y., 1983; F. Weber and N. K. Glendenning, astro-ph/9609074, 1996.

[95] N.K. Glendenning, COMPACT STARS, *Nuclear Physics, Particle Physics, and General Relativity* (Springer-Verlag, 1997).

[96] K. Schertler, C. Greiner and M.H. Thoma, Nucl. Phys. **A616**, 659 (1997).

[97] V. Goloviznin and H. Satz, Z. Phys. **C57** 671 (1993); A. Peshier et al, Phys. Lett. **B337** 235 (1994).

[98] A. Peshier et al, Phys. Rev. **D54** 2399 (1996).

[99] V.V. Klimov, Sov. Phys. JETP **55** (1982) 199; H.A. Weldon Phys. Rev. **D26** (1982) 1394 and 2789 (1982); H. Vija and M.H. Thoma, Phys. Lett. **B342** (1995) 212; J.-P. Blaizot and J.-Y. Ollitrault, Phys. Rev. **D48** (1993) 1390.

[100] J. R. Oppenheimer and G. M. Volkoff, Phys. Rev. **55**, 374 (1939).

[101] N. K. Glendenning and F. Weber, Astrophys. J **400**, 647 (1992); C.J. Pethick and D.G. Ravenhall, Annu. Rev. Nucl. Part. Sci. **45**, 429 (1995).

[102] K. Schertler, C. Greiner, P.K. Sahu and M.H. Thoma, ‘The influence of medium effects on the gross structure of hybrid stars’, astro-ph/9712165.

- [103] N.K. Glendenning, Phys. Rev. **D46**, 1274 (1992).
- [104] We thank K. Schertler for providing us with Fig. 30.
- [105] N.K. Glendenning, Astrophys. J. **293**, 470 (1985).
- [106] D.B. Kaplan and A.E. Nelson, Phys. Lett. **B175**, 57 (1986); A.E. Nelson and D.B. Kaplan, Phys. Lett. **B192**, 193 (1987).
- [107] G.E. Brown, K. Kubodera, M. Rho and V. Thorsson, Phys. Lett. **B291**, 355 (1992); V. Thorsson, M. Prakash and J.M. Lattimer, Nucl. Phys. **A572**, 693 (1994); G.E. Brown, C.-H. Lee, M. Rho and V. Thorsson, Nucl. Phys. **A567**, 937 (1994); C.-H. Lee, G.E. Brown, D.-P. Min and M. Rho, Nucl. Phys. **A585**, 401 (1995).
- [108] P.J. Ellis, R. Knorren and M. Prakash, Phys. Lett. **B349**, 11 (1995); R. Knorren, M. Prakash and P.J. Ellis, Phys. Rev. **C52**, 3470 (1995).
- [109] J. Schaffner and I.N. Mishustin, Phys. Rev. **C53**, 1416 (1996).
- [110] H. Fujii, T. Maruyama, T. Muto and T. Tatsumi, Nucl. Phys. **A597**, 645 (1996).
- [111] G.E. Brown and H.A. Bethe, Astrophys. J. **423**, 659 (1994).
- [112] T. Maruyama, H. Fujii, T. Muto and T. Tatsumi, Phys. Lett. **B337**, 19 (1994).
- [113] J. Schaffner, A. Gal, I.N. Mishustin, H. Stöcker and W. Greiner, Phys. Lett. **B334**, 268 (1994).

This figure "fig1-1.png" is available in "png" format from:

<http://arxiv.org/ps/nucl-th/9801062v1>

This figure "fig1-2.png" is available in "png" format from:

<http://arxiv.org/ps/nucl-th/9801062v1>

This figure "fig1-3.png" is available in "png" format from:

<http://arxiv.org/ps/nucl-th/9801062v1>

This figure "fig1-4.png" is available in "png" format from:

<http://arxiv.org/ps/nucl-th/9801062v1>

This figure "fig1-5.png" is available in "png" format from:

<http://arxiv.org/ps/nucl-th/9801062v1>

This figure "fig1-6.png" is available in "png" format from:

<http://arxiv.org/ps/nucl-th/9801062v1>